A numerical transcendental method in algebraic geometry: Computation of Picard groups and related invariants

Pierre Lairez, Emre Can Sertöz

A numerical transcendental method in algebraic geometry: Computation of Picard groups and related invariants

Pierre Lairez* and Emre Can Sertöz†

Abstract. Based on high precision computation of periods and lattice reduction techniques, we compute the Picard group of smooth surfaces in $\mathbb{P}^3$. As an application, we count the number of rational curves of a given degree lying on each surface. For quartic surfaces we also compute the endomorphism ring of their transcendental lattice. The method applies more generally to the computation of the lattice generated by Hodge cycles of middle dimension on smooth projective hypersurfaces. We demonstrate the method by a systematic study of thousands of quartic surfaces (K3 surfaces) defined by sparse polynomials. The results are only supported by strong numerical evidence; yet, the possibility of error is quantified in intrinsic terms, like the degree of curves generating the Picard group.

1. Introduction.

Griffiths emphasized the role of certain multivariate integrals, known as *periods*, "to construct a continuous invariant of arbitrary smooth projective varieties" [39]. Periods often determine the projective variety completely and therefore its algebraic invariants. Translating periods into discrete algebraic invariants raises difficult questions, exemplified by the long standing Hodge conjecture which describes how periods determine the algebraic cycles within a projective variety.

Recent progress in computer algebra makes it possible to compute periods with high precision [68] and put transcendental methods into practice. This opens new possibilities in numerical algebraic geometry. While path tracking methods from numerical algebraic geometry are successful at computing topological invariants—irreducible decomposition [71], monodromy groups [43] or Chern numbers [25]—the computation of periods reveal finer algebraic invariants. For example, they are used to compute the endomorphism ring of the Jacobian variety of algebraic curves [79, 7, 21, 12]. We extend this transcendental method to higher dimensions and focus mainly on algebraic surfaces. We describe and implement a numerical method to compute Picard groups of smooth surfaces. As an application, we count smooth rational curves on quartic surfaces using the Picard group. We demonstrate that these methods apply more generally to smooth hypersurfaces in a projective space of arbitrary dimension. Throughout the paper we work over the complex field but the implementation is for hypersurfaces defined over the rationals.

Structure of the Picard group and main results.

There are many curves in a smooth surface $X \subset \mathbb{P}^3$. The basic ones are those obtained by intersecting X with another surface S in $\mathbb{P}^3$. If S_1 and S_2 are two surfaces of the same degree then the curve $C_1 = S_1 \cap X$ can be deformed into the curve $C_2 = S_2 \cap X$ by varying continuously the coefficients of the defining equation of S_1. The curves C_1 and C_2 are said to be *linearly equivalent*. The notion of linear equivalence extends to formal $\mathbb{Z}$-linear combinations of curves and the Picard group [40, p. 143]

*Inria, France
†Max Planck Institute MiS, Leipzig, Germany

of X is defined by

$$\mathrm{Pic}(X) \stackrel{\text{def}}{=} \mathbb{Z}\langle \text{algebraic curves in } X\rangle / \langle \text{linear equivalence relations}\rangle.$$

The Picard group is an algebraic invariant that reflects the nature of the algebraic curves lying on X. It is a free abelian group, that is, $\mathrm{Pic}(X) \simeq \mathbb{Z}^\rho$ for a positive integer ρ called the *Picard number* of X. As Zariski wrote, "The evaluation of ρ for a given surface presents in general grave difficulties" [83, p. 110].

There is more to the Picard group than the Picard number. The intersection product, which for any two curves C_1 and C_2 in X associates an integer $C_1 \cdot C_2$, induces a bilinear map $\mathrm{Pic}(X) \times \mathrm{Pic}(X) \to \mathbb{Z}$. The intersection product is an intrinsic algebraic invariant of X that is finer than the Picard number. There is also an extrinsic invariant in the Picard group, called the *polarization*, recording much of the geometry of X within $\mathbb{P}^3$. The polarization is the linear equivalence class of any curve obtained by intersecting X with a plane in $\mathbb{P}^3$. The problem we address is then the following: *Given the defining equation of X, compute the Picard number ρ of X, the $\rho \times \rho$ matrix of the intersection product and the ρ coordinates of the polarization in some basis of* $\mathrm{Pic}(X) \simeq \mathbb{Z}^\rho$.

We approach the problem using *transcendental methods*, that is, we use the complex geometry of the hypersurfaces and compute multivariate integrals on topological cycles, namely the *periods*. For surfaces, the Lefschetz $(1,1)$ theorem identifies the Picard group of a surface with the lattice of integer linear relations between periods. The rank, intersection product and polarization of the Picard group can be computed from a high precision computation of the periods [68] and well-established techniques in lattice reduction. We apply these techniques also to the computation of the endomorphism ring of the transcendental lattice in order to compute Charles's gap [14], see below. Counting rational curves of a given degree lying on a surface is an interesting application of the computation of the Picard group with its intersection product and polarization. We study rigorously the reliability of using approximate periods to make deductions about integral relations between them. In addition, we built a database containing $180,000$ quartic surfaces to demonstrate the feasibility of the approach.

The method extends to higher dimensional hypersurfaces in order to compute the group of Hodge cycles. For a hypersurface X in a projective space of odd dimension $\mathbb{P}^{2k+1}_{\mathbb{C}}$ with $k > 1$ there are two interesting objects to study, replacing the Picard group for surfaces under present discussion: the group of algebraic cycles $\mathrm{Alg}^k(X)$ generated by the cohomology classes of k-dimensional algebraic subvarieties of X or the group of Hodge cycles $\mathrm{Hdg}^k(X)$ generated by integral linear relations between periods. The Hodge conjecture states in greater generality that, after tensoring with rational numbers, the two groups $\mathrm{Alg}^k(X) \otimes_{\mathbb{Z}} \mathbb{Q}$ and $\mathrm{Hdg}^k(X) \otimes_{\mathbb{Z}} \mathbb{Q}$ coincide [24]. The resolution of this conjecture is one of the seven Millennium Prize Problems posed by the Clay Institute. Perhaps the current method will allow for experimentation in this direction with the ability to compute $\mathrm{Hdg}^k(X)$ together with its intersection product and polarization, see §5.

Applications. Let X be the space of solutions to a polynomial system of equations, as might occur in integer programming, algebraic statistics or geometric modeling. It is natural to consider subspaces of solutions that can be freely parametrized algebraically, such as linear spaces inside X. When $X \subset \mathbb{P}^3$ is a smooth quartic surface, there is no dominant rational map

$\mathbb{P}^2 \dashrightarrow X$ but there are often non-constant maps $\mathbb{P}^1 \to X$. One of the applications of having the Picard group of a quartic surface is the immediate ability to count smooth rational curves, i.e. embeddings $\mathbb{P}^1 \hookrightarrow X$, of any degree, see §3. Symbolic methods can tackle this problem too but to the best of our knowledge, the computational complexity is too high to count anything else that curves of degree one or two. Attempts at counting the number of maps $\mathbb{P}^1 \to X$ led to deep connections between mathematics, string theory and mirror symmetry [44].

Periods of curves play a crucial role in finding algebro-geometric solutions to soliton equations, e.g. integrable models in the KdV hierarchy. There is a large amount of work, theoretical and applied, building upon this connection [70, 37, 22]. It is conceivable that periods of higher dimensional varieties, now that they are easily accessible, will find new applications.

Numerical period computations are used in constructing higher terms in Feynman integrals appearing in perturbative quantum field theory [80, 10, 74]. Interpretations of the numerical periods as rational linear sums of some expected transcendental numbers play an important role in understanding the structure of these numbers [10]. A better understanding of the reasons underlying this expected decomposition led to a surprising connection between high energy physics and number theory [74]. Of direct relevance to our work is the paper [35] A concrete application of computing Picard group of K3 surfaces is the proof of the impossibility of resolving a square root in the parametrization of a two-loop Feynman integral [35].

Beyond physical interpretations, the behavior of periods is described in the global framework of motives developed in the past decade [11]. The tools we develop open new ways of experimentation. The computation of the Picard number of K3 surfaces in particular play a crucial role in understanding the dimension of the mirror family associated to a given K3 surface [26]: computing the lattice structure of the Picard group gives an exact determination for the base of this mirror family.

To further develop number theory as well as its applications to physics and cryptography the LMFDB (The L-functions and Modular Forms Database) [72] was constructed (see also [1]), partially relying on period computations of curves [54, 21]. The numerical transcendental method introduced in our work applies well enough to surfaces to allow generation of databases of similar nature[1].

Related work. For surfaces of degree at most three the Picard group does not depend on the defining equations and the main arguments to compute it have been known since the 19th century [27]. Starting with surfaces of degree four, the Picard group is sensitive to the defining equations and its computation poses an entirely different kind of challenge. Noether and Lefschetz [52] proved that a very general quartic surface has Picard number one. However, the first quartic with $\rho = 1$ defined by a polynomial with integer coefficients appeared in 2007 with van Luijk's seminal paper [78] where he used techniques involving reduction to finite characteristic. Since then the reduction techniques have been going through a phase of rapid development. The original argument of van Luijk was refined by Elsenhans and Jahnel [29, 28] but the computational bottleneck persisted: in working with surfaces over finite fields the computation of their Zeta function initially required the expensive process of point

[1] A proof-of-concept database containing more that 180,000 quartic surfaces is available at https://pierre.lairez.fr/quarticdb.

counting. This bottleneck has been alleviated using ideas from p-adic cohomology and gave rise to two different approaches: one dealing directly with the surface [48, 2, 20] and another which deforms the given surface to a simpler one [51, 62].

To complement the upper bounds coming from prime reductions, lower bounds on the Picard number can be obtained, at least in theory, by enumerating all the algebraic curves in X. One could compute infinite sequences of lower and upper bounds that may eventually determine the Picard number. However, Charles [14] proved that the upper bounds obtained from finite characteristic could significantly overestimate the Picard number and he expressed the gap in terms of the endomorphism ring of the transcendental lattice, see §2.3. In practice, computing this gap appears to be just as difficult as the computation of the Picard number. However, Charles demonstrated at last that the Picard number of a K3 surface (e.g. a quartic surface) defined with coefficients in a number field is computable. On the theoretical side, effective algorithms have been developed with a broader reach but with low practicability [14, 41, 65]. There is recent work addressing the issue of practicability [34].

Concerning numerical methods, high precision computation of periods has been successfully applied to many problems concerning algebraic curves [79, 12], even with the possibility of *a posteriori* symbolic certification [21].

Tools. For the purpose of exposition, we focus mainly on quartic surfaces. Our techniques, as well as our code, work for hypersurfaces of any degree and dimension, given sufficient computational resources. The main computational tool on the one hand is an algorithm to approximate periods [68], based on Picard–Fuchs differential equations [64], algorithms to compute them, [17, 49, 61, 59, 50, 9], and numerical analytic continuation [77, 76, 16, 56, 57]. On the other hand, we use algorithms to compute integer linear relations between vectors of real numbers [33, 53, 42, 13, 32, 15].

We used the computer algebra system SageMath [73] with *ore_algebra-analytic*[2] [57] for performing numerical analytic continuation and our code base is bundled as *numperiods*.[3] Early experiments have been performed in Magma [8], with *PeriodSuite*[4] [68] and *periods*[5] [50].

The reliability of numerical computations. Although the periods vary continuously with the coefficients of the defining equation of a surface, the Picard number is nowhere continuous for surfaces of degree at least 4 [18] and behaves like the indicator function of the rational numbers on the real line. This suggests that finite precision approximations of the periods of a surface are not enough to formally determine the Picard group. Although sufficiently high precision will compute the Picard group correctly, we do not know what precision is sufficient.

Instead, given the precision of the computation we determine a number B such that the computed lattice contains the sublattice of the Picard group generated by all elements of norm at most B. For example, using 600 decimal digits we have typically $B \sim 10^{100}$. In terms of degree, it means that the group we compute contains all curves of degree at most B. With over 180,000 examples, we never observed a generator of norm > 100. On the other extreme, small relations may yield periods that are 0 to 600 decimal places but are non-zero. Such a

[2] http://marc.mezzarobba.net/code/ore_algebra-analytic
[3] https://gitlab.inria.fr/lairez/numperiods
[4] https://github.com/emresertoz/PeriodSuite
[5] https://github.com/lairez/periods

numerical coincidence would invalidate the computation by introducing false generators into the lattice. We quantify the possibility of these errors precisely and relate them to quantities intrinsic to the surface, see §4. If these intrinsics of the surface could be computed they would allow for the certification of the numerical computations, however this computation appears out of reach.

We checked our results against the literature whenever possible. In particular, we compared our Picard number computations against *controlledreduction*[6] [19] and Shioda's algorithm for Delsarte surfaces defined by a sum of four monomials [69]. Whenever a check was possible, our computations gave the correct result.

Outline. In Section 2, we describe the computation of the Picard group of surfaces and the endomorphism ring of the transcendental lattice of quartic surfaces from an approximation of periods. In Section 3 we apply our computations to count smooth rational curves in quartic surfaces. In Section 4 we describe and analyze a standard procedure to recover integer relations between approximate real vectors. We quantify the nature of error in a way that is independent of the methods employed and express it in terms of an intrinsic measure of complexity of the given surface. Section 5 explains the situation for higher dimensional hypersurfaces where the general idea of the method as explained in Section 2 applies verbatim. Section 6 summarizes the experimental results obtained for over thousands of quartic surfaces. Section 7 explains how we compute the polarization by fleshing out the argument given in [68].

Acknowledgments. We would like to thank Bernd Sturmfels for putting us together, for his guidance and constant support. We also would like to thank Alex Degtyarev for explaining to us how to count rational curves in a K3 lattice. We are also grateful for insightful conversations with Simon Brandhorst, John Cannon, Edgar Costa, Stephan Elsenhans, Jon Hauenstein, Marc Mezzarobba, Mateusz Michałek, Matthias Schütt and Don Zagier, and for the valuable comments of the referees.

2. Periods and Picard group.

2.1. Principles. Following Picard, Lefschetz and Hodge, algebraic curves on a smooth complex surface X can be characterized among all topological 2-dimensional cycles of X in terms of multivariate integrals (for a historical perspective, see [58, 45]).

Let $X \subset \mathbb{P}^3$ be a smooth complex surface. An algebraic curve $C \subset X$ is supported on a topological 2-dimensional cycle. Lefschetz proved that two algebraic curves are topologically homologous if and only if they are linearly equivalent [52], see also [58, Chap. 9]. In other words, the Picard group comes with a natural inclusion into the homology group

$$\mathrm{Pic}(X) \hookrightarrow H_2(X, \mathbb{Z}). \tag{2.1}$$

This homology group is a topological invariant that depends only on the degree of X, while $\mathrm{Pic}(X)$ is a much finer invariant of X.

Recall that for a 2-dimension cycle γ and any holomorphic differential 2-form ω on X, the integral $\int_\gamma \omega$ is well defined on the homology class of γ.

[6] https://github.com/edgarcosta/controlledreduction

Theorem 2.1 (The Lefschetz (1,1) theorem). *A homology class $\gamma \in H_2(X,\mathbb{Z})$ is in* $\mathrm{Pic}(X)$ *if and only if $\int_\gamma \omega = 0$ for every holomorphic 2-form ω on X.*

When X has degree 4, $H_2(X,\mathbb{Z}) \simeq \mathbb{Z}^{22}$ and X admits a unique non-zero holomorphic 2-form up to scaling, which we denote ω_X. Given a basis $\gamma_1, \ldots, \gamma_{22}$ of $H_2(X,\mathbb{Z})$, Theorem 2.1 becomes

$$\mathrm{Pic}(X) = \left\{ (a_1, \ldots, a_{22}) \in \mathbb{Z}^{22} \;\middle|\; \sum_{i=1}^{22} a_i \int_{\gamma_i} \omega_X = 0 \right\}. \tag{2.2}$$

The integrals $\int_{\gamma_i} \omega_X$ appearing here are called the *periods* of X. All periods can be expressed as a sum of integrals in the affine chart $\mathbb{C}^3 = \{w = 1\} \subset \mathbb{P}^3$. For a 2-cycle $\gamma \subset X \cap \{w = 1\}$ we can form a thin tube $\tau \subset \mathbb{C}^3 \setminus X$ around γ so that

$$\int_\gamma \omega_X = \frac{1}{2\pi\sqrt{-1}} \int_\tau \frac{\mathrm{d}x\,\mathrm{d}y\,\mathrm{d}z}{f(x,y,z,1)}, \tag{2.3}$$

where f is the degree 4 homogeneous polynomial defining X [38].

In general, when X has degree $d \geq 4$, $H_2(X,\mathbb{Z})$ has rank $m = d^3 - 4d^2 + 6d - 2$ and the space $\Omega^2(X)$ of holomorphic 2-forms on X is of dimension $r = \binom{d-1}{3}$. Fixing bases $H_2(X,\mathbb{Z}) = \mathbb{Z}\langle\gamma_1, \ldots, \gamma_m\rangle$, $\Omega^2(X) = \mathbb{C}\langle\omega_1, \ldots, \omega_r\rangle$ and applying Lefschetz (1,1) theorem we get:

$$\mathrm{Pic}(X) = \left\{ (a_1, \ldots, a_m) \in \mathbb{Z}^m \;\middle|\; \forall 1 \leq j \leq r, \sum_{i=1}^{m} a_i \int_{\gamma_i} \omega_j = 0 \right\}. \tag{2.4}$$

In view of (2.2) and (2.4) we can determine $\mathrm{Pic}(X)$ by computing the matrix of periods $\mathcal{P} = (\int_{\gamma_j} \omega_i)_{i,j}$ and then finding integer linear relations between the rows, that is, by computing the integral right kernel of $\mathcal{P}$. The algorithm presented in [68] to compute the periods of X takes care of the first step. We may then use lattice reduction algorithms [53, p. 525] to find generators for $\mathrm{Pic}(X)$.

We briefly recall how periods of X are computed in [68]. The surface X is put into a single parameter family of surfaces containing the Fermat surface $Y = \{x^d + y^d + z^d + w^d = 0\}$. The matrix of periods along the family vary holomorphically in terms of the parameter and these entries satisfy ordinary differential equations which are computed exactly, the Picard-Fuchs differential equations. The value of this one parameter period matrix—as well as its derivatives—at Y are given by formulas involving Gamma functions. The differential equations together with the periods on Y expresses the periods of X as the solution to an initial value problem. This initial value problem is solved using Mezzarobba's implementation of numerical analytic continuation [57] to arbitrary precision with rigorous error bounds.

The reconstruction of integer relations between numbers that are only approximately given is not possible in general. However, we can guess generators of the integer relations, and prove that these putative generators are genuine generators when the precision is high enough. Section 4 is devoted to the study of this problem.

0	0	0	0	0	0	0	0	0	0	0	0	0	0	−1669083212117905913652734	0	1937019641160560221317687	...
0	0	0	0	0	0	0	0	0	0	0	0	0	0	0	1669083212117905913652734	1937019641160560221317687	...
1	0	0	−1	0	0	0	1	1	0	0	0	0	0	−146511829901195443671789	84478429044587822467823	−365980228690630104919296	...
0	0	0	0	1	0	0	0	0	0	0	0	0	0	−337167720252678310258177	224110151973403946221421	−743116955936487279910552	...
0	0	0	0	0	0	0	0	0	0	0	0	1	−1	357031479253522311483650	768066337666351099432748	940525994719391079998435	...
0	0	0	0	0	1	0	0	1	0	1	0	0	0	−552756671828854153114905	−126018248279583585486071	535095811953165917210863	...
0	−1	1	0	0	0	0	0	1	0	0	−1	0	0	104335431129908645825133	−231616284585318363570849	502730408585962411025306	...
0	0	0	0	0	0	0	0	0	0	0	0	0	−1	−649159586430203173692632	770784867967071100945665	−2152014469737999315531272	...
0	0	0	0	0	0	0	0	0	1	1	0	0	0	277747983934797690835205	−28625739873061372966384	−638732179408358479990097	...
1	0	0	0	0	0	0	0	0	0	0	1	0	0	146511829901195443671790	−84478429044587822467823	365980228690630104919296	...
0	0	0	0	0	0	0	0	0	0	0	−1	1	1	250899146775406645936761	575615030011256031395007	−114830012426104078247291	...
0	1	0	0	0	0	0	1	0	0	−1	0	0	0	104335431129908645825133	−231616284585318363570849	502730408585962411025307	...
0	0	0	0	0	0	−1	0	0	0	0	0	1	−1	−140644950443454586919439	−393058206212350140614235	429933080833930208291557	...
0	0	0	0	0	0	0	0	1	0	0	0	0	0	594933070600140950961561	273156103820314126589096	−671845991848498223316874	...
0	0	0	0	1	0	0	−1	0	0	0	0	0	0	337167720252678310258177	−224110151973403946221421	743116955936487279910552	...
0	0	0	0	0	0	0	0	0	0	0	0	0	1	−824317154838996681984621	177119763197465887754938	−236792300924643740702432	...
0	0	0	0	0	0	0	1	0	0	1	0	0	0	379344119023965108104833	−76972296432673405118395	606366776041154973804541	...
0	0	0	0	0	1	0	0	0	0	0	0	0	0	552756671828854153114905	126018248279583585486070	−535095811953165917210864	...
0	0	0	0	0	0	1	0	0	0	0	0	0	−1	−140644950443454586919440	−393058206212350140614234	429933080833930208291557	...
0	0	1	0	0	0	0	0	0	0	0	0	0	0	−104335431129908645825133	231616284585318363570849	−502730408585962411025307	...
0	0	0	0	0	0	0	0	0	0	0	0	1	0	−467285675585474370500971	−950623161465256990213520	−1255629063127217210042702	...
0	0	0	1	0	0	0	0	0	0	0	0	0	0	−146511829901195443671790	84478429044587822467823	−365980228690630104919296	...
0	0	0	0	0	0	0	0	0	1	0	−1	0	0	−277747983934797690835206	28625739873061372966384	638732179408358479990097	...
0	0	0	0	0	0	0	0	0	0	0	1	0	0	−69025235930677842745100	457102914343586863258366	660652346877586707848817	...

Figure 2.1. *Lattice of integer relations between approximate periods. The last 5 columns are omitted.*

2.2. An example. Consider the quartic surface $X \subset \mathbb{P}^3$ defined by the polynomial

$$f = 3x^3z - 2x^2y^2 + xz^3 - 8y^4 - 8w^4. \tag{2.5}$$

As described above, we may compute a 1×22 matrix of periods to arbitrary precision. In this example, the differential equations that arise are of order 5 with polynomial coefficients of degree at most 59. On a laptop, the determination of this differential equation takes about two seconds and it takes 30 seconds to integrate it to 100 digits of accuracy, with rigorous error bounds.

Applying the LLL algorithm to these approximate periods of X gives a basis of integer relations between the approximate periods. More precisely, we consider for the lattice Λ of integer vectors $(u, v, a_1, \ldots, a_{22}) \in \mathbb{Z}^{24}$ satisfying

$$\sum_{i=1}^{22} a_i \left[10^{100} \int_{\gamma_i} \omega_X \right] = u + v\sqrt{-1}, \tag{2.6}$$

where $[-]$ denotes the rounding of real and imaginary part to nearest integer. Equation (2.6) should be compared with (2.2). Short vectors in $\mathrm{Pic}(X)$ give rise to short vectors in Λ, and a short vector in Λ is likely to come from a vector in $\mathrm{Pic}(X)$, unless a surprising numerical cancellation happens.

Concerning the example, Figure 2.1 shows a matrix whose columns form a LLL-reduced basis for the lattice Λ. We observe an important gap in size, between the 14th and 15th column. We infer that the Picard number of X is 14 and that the columns of the lower left 22×14 submatrix is a basis of $\mathrm{Pic}(X)$. The norm of the first dismissed column, about 10^{25}, fits precisely the expected situation described in Proposition 4.3.

This numerical approach may fail in two ways: either by missing a relation or by returning a false relation which nevertheless holds up to high precision. Proposition 4.1 quantifies the

$$\begin{bmatrix}
-4 & 0 & 0 & 2 & 2 & 2 & 0 & -3 & -1 & -2 & 0 & -1 & 1 & -1 \\
0 & -4 & 2 & 0 & -1 & 1 & 2 & -1 & 2 & 0 & 4 & -2 & 0 & 0 \\
0 & 2 & -4 & 0 & 2 & 0 & -2 & -1 & -1 & 0 & 0 & 2 & 1 & -1 \\
2 & 0 & 0 & -4 & -1 & -1 & 0 & 3 & 2 & 0 & 0 & 0 & 0 & 0 \\
2 & -1 & 2 & -1 & -4 & 0 & 1 & 3 & 1 & 2 & 1 & 0 & -1 & -1 \\
2 & 1 & 0 & -1 & 0 & -4 & -1 & 1 & -1 & 2 & -3 & -1 & 1 & 3 \\
0 & 2 & -2 & 0 & 1 & -1 & -4 & 1 & -2 & 0 & -2 & 0 & 2 & 2 \\
-3 & -1 & -1 & 3 & 3 & 1 & 1 & -6 & -1 & -1 & 1 & 0 & 1 & -1 \\
-1 & 2 & -1 & 2 & 1 & -1 & -2 & -1 & -4 & 1 & -2 & 0 & 2 & 0 \\
-2 & 0 & 0 & 0 & 2 & 2 & 0 & -1 & 1 & -4 & 0 & 1 & -1 & 1 \\
0 & 4 & 0 & 0 & 1 & -3 & -2 & 1 & -2 & 0 & -10 & -1 & 0 & 3 \\
-1 & -2 & 2 & 0 & 0 & -1 & 0 & 0 & 0 & 1 & -1 & -6 & 2 & 3 \\
1 & 0 & 1 & 0 & -1 & 1 & 2 & 1 & 2 & -1 & 0 & 2 & -4 & 0 \\
-1 & 0 & -1 & 0 & -1 & 3 & 2 & -1 & 0 & 1 & 3 & 3 & 0 & -10
\end{bmatrix}
\quad
\begin{bmatrix}
-4 \\ -5 \\ 0 \\ -2 \\ 4 \\ 3 \\ 1 \\ 3 \\ -1 \\ 6 \\ -2 \\ 4 \\ 0 \\ 2
\end{bmatrix}$$

Figure 2.2. *Matrix of the intersection product and the coordinates of the hyperplane section in* $\mathrm{Pic}(X)$.

way in which such a failure may occur: either the computation of $\mathrm{Pic}(X)$ is correct; or $\mathrm{Pic}(X)$ is not generated by elements of norm $< 10^{20}$; or there is some $(a_i) \in \mathbb{Z}^m$ with $\sum_i a_i^2 \leq 4$ such that $\left|\sum_i a_i \int_{\gamma_i} \omega_X\right|$ is not zero but smaller than 10^{-99}. Section 4.2 expresses these quantities independently of any choice occurring in the computation.

The intersection product on $\mathrm{Pic}(X)$ is readily computed from the generators, as we now describe. The basis of homology on X is obtained by carrying a basis from the Fermat surface Y by parallel transport. On Y the intersection numbers $\gamma_i \cdot \gamma_j$ are known exactly as well as the polarization, i.e. the coordinates of the homology class of a general place section $H \cap X$ in the basis $\{\gamma_i\}_{i=1}^{22}$, see §7. As these values remain constant during parallel transport, we know the intersection product on the homology of X as well as the polarization. Computing the intersection product of the 14 generators of $\mathrm{Pic}(X)$ in homology, we obtain the intersection product on $\mathrm{Pic}(X)$. Since the polarization lies in $\mathrm{Pic}(X)$ we express it in terms of these generators of $\mathrm{Pic}(X)$. The result of this operation is displayed in Figure 2.2.

Applying standard methods to be discussed in §3, we find from the Picard lattice of X that there are 4 lines, 102 quartic curves and no twisted cubics inside X.

2.3. Transcendental lattice and reduction to finite characteristic.

Definition and properties. Let X be a quartic surface. Beyond the Picard group of X, we can compute its *transcendental lattice* and its *endomorphism ring*. The transcendental lattice of X is given by

$$T \stackrel{\text{def}}{=} \left\{\omega \in H^2(X,\mathbb{Z}) \;\middle|\; \forall \gamma \in \mathrm{Pic}(X), \omega \cdot \gamma = 0\right\}. \tag{2.7}$$

We will denote the associated spaces by $T_{\mathbb{Q}} = T \otimes \mathbb{Q}$ and $T_{\mathbb{C}} = T \otimes \mathbb{C}$. Observe that $\omega_X \in T_{\mathbb{C}} \subset H^2(X,\mathbb{C})$ by (2.2). The endomorphism ring E is defined as the subring of all $\mathbb{Q}$-linear maps $e\colon T_{\mathbb{Q}} \to T_{\mathbb{Q}}$ preserving the intersection product and satisfying $e(\omega_X) \in \mathbb{C}\langle\omega_X\rangle$, for the canonical extension of e to $H^2(X,\mathbb{C})$. The map $\varphi\colon E \to \mathbb{C}$ defined by $e(\omega_X) = \varphi(e)\omega_X$ is an injective ring morphism and every nonzero element in E is invertible, therefore E is

a number field [46, Corollary 3.3.6]. In fact, E is either totally real or a CM-field [82], see also [46].

Charles [14] determined in terms of E the overestimation of reduction methods to compute the Picard number of K3 surfaces. We give here a quick overview, see [46, 75] for further results. Although we state these results for quartic surfaces over $\mathbb{Q}$ much of it holds for any K3 surface over a number field.

If the quartic $X \subset \mathbb{P}^3$ is defined by a polynomial f with integer coefficients, we may consider for all but finitely many prime p the smooth quartic surface X_p defined over $\mathbb{F}_p$ by the reduction of f modulo p. Let ρ and ρ_p denote the (geometric) Picard numbers of X and X_p respectively. Let ρ_{red} be the minimum of the set $\{\rho_p \mid p > 5 \text{ prime and } X_p \text{ smooth}\}$. The starting point of reduction methods is the inequality $\rho \leq \rho_{\mathrm{red}}$ and the relative ease with which the numbers ρ_p are computed. A key issue is to determine whether $\rho = \rho_{\mathrm{red}}$.

Although ρ can be either even or odd, ρ_p is always even. This issue was partially overcome by van Luijk [78] who gave necessary conditions for $\rho = \rho_{\mathrm{red}}$. He used his argument to give the first example of a K3 surface defined over the rationals with Picard number 1 by exhibiting a surface X with $\rho_{\mathrm{red}} = 2$ that does not satisfy his necessary condition. It was asked by Elsenhans and Jahnel [30] whether $\rho = \rho_{\mathrm{red}}$ if ρ is even and $\rho = \rho_{\mathrm{red}} - 1$ if ρ is odd. Charles [14] settled the question in the negative.

Theorem 2.2 (Charles). *The equality $\rho_{\mathrm{red}} = \rho$ holds unless E is totally real and the dimension of $T_{\mathbb{Q}}$ over E is odd, in which case $\rho_{\mathrm{red}} = \rho + \dim_{\mathbb{Q}} E$.*

Computation. From the numerical computation of periods, we obtain approximations of $a_i \overset{\text{def}}{=} \int_{\gamma_i} \omega_X \in \mathbb{C}$ for some basis $\gamma_1, \ldots, \gamma_{22}$ of $H_2(X, \mathbb{Z})$. The cohomology group $H^2(X, \mathbb{C})$ is endowed with the dual basis $\gamma_1^*, \ldots, \gamma_{22}^*$ so that $\omega_X = \sum_i a_i \gamma_i^*$. Once a basis $u_1, \ldots, u_\rho$ of the Picard group $\mathrm{Pic}(X)$ is computed, a basis $v_1, \ldots, v_{\rho'}$ of $T = \mathrm{Pic}(X)^\perp \subseteq H^2(X, \mathbb{Z})$ is found readily. Let us remark that during our computations, the intersection products $\gamma_i^* \cdot \gamma_j^*$ are known exactly and therefore the intersection product on T is immediately deduced.

For $e \in \mathrm{End}_{\mathbb{Q}}(H^2(X, \mathbb{Q}))$ the condition $e \in E$ can be rewritten as:

$$\exists \lambda \in \mathbb{C} : e(\omega_X) = \lambda \omega_X \Leftrightarrow \langle \omega_X, e(\omega_X) \rangle \omega_X = \langle \omega_X, \omega_X \rangle e(\omega_X). \tag{2.8}$$

Writing $A = (a_1, \ldots, a_{22})^t$ for the coefficient vector of ω_X, we can compute the endomorphism ring E via the following formulation:

$$E = \mathbb{Q} \cdot \left\{ M \in \mathbb{Z}^{\rho' \times \rho'} \;\middle|\; (\bar{A}^t M A) A = (\bar{A}^t A) M A \right\}. \tag{2.9}$$

Just as with the computation of $\mathrm{Pic}(X)$, the problem of computing E is now a problem of computing integer solutions to linear equations with approximate real coefficients. We approach it once again with lattice reduction algorithms, see §4. Examples are provided in §6.

3. Smooth rational curves in K3 surfaces. The data of the matrix of the intersection product in some basis of the Picard group of a smooth quartic surface $X \subset \mathbb{P}^3$ together with the coordinates of the class of hyperplane section in the same basis (as in Figure 2.2) is enough to count all smooth rational curves of a given degree lying on X.[7] In principle, smooth rational

[7] We are indebted to Alex Degtyarev for sharing his understanding with us.

curves in a surface can be enumerated using purely symbolic methods and for lines this process is routine. However, it is a challenge to enumerate even the quadric curves in quartic surfaces, let alone higher degree curves in higher degree surfaces. The computation of the Picard group offers an indirect solution to this problem.

Fix a smooth quartic $X \subset \mathbb{P}^3$ and for each positive integer d let $\mathcal{R}_d$ be the set of all smooth rational curves of degree d lying in X. In order to compute the cardinality of the set $\mathcal{R}_d$ we will first observe that a smooth rational curve is completely determined by its linear equivalence class. Recall that we denote by $h_X \in \mathrm{Pic}(X)$ the class of a hyperplane section. For $d > 0$ we define the set $M_d = \left\{ D \in \mathrm{Pic}(X) \;\middle|\; D^2 = -2,\ D \cdot h_X = d \right\}$.

Lemma 3.1. *A smooth rational curve in X is isolated in its linear equivalence class. Moreover, the map $\mathcal{R}_d \to \mathrm{Pic}(X)$ which maps a rational curve to its linear equivalence class injects $\mathcal{R}_d$ into M_d.*

Proof. Let $C \in \mathcal{R}_d$ and $D = [C] \in \mathrm{Pic}(X)$. As C is of degree d, it intersects a general hyperplane in d points so that $C \cdot h_X = d$. Recall that the canonical class K_X of the K3 surface X is trivial so that adjunction formula reads $D^2 = D \cdot (K_X + D) = 2g(\mathbb{P}^1) - 2 = -2$ [6, §II.11][40, Ex. V.1.3]. This proves that the image of $\mathcal{R}_d$ lies in M_d.

Now we show that C is isolated in its linear system. Indeed, if C' is a curve linearly equivalent to but different from C, then the intersection number $[C] \cdot [C']$ must be positive, as this number can be obtained by counting the points in $C \cap C'$ with multiplicity. This leads to a contradiction: $-2 = [C]^2 = [C] \cdot [C'] > 0$. ∎

Typically, the inclusion $\mathcal{R}_d \hookrightarrow M_d$ is strict. We now demonstrate that with knowledge of $M_{d'}$ for each $d' \leq d$ one can compute the image of $\mathcal{R}_d$ in M_d. For each $d > 0$ define inductively a subset $N_d \subset M_d$ as follows:

$$N_d = \left\{ D \in M_d \;\middle|\; \forall d' < d, \forall D' \in N_{d'}, D' \cdot D \geq 0 \right\}. \tag{3.1}$$

Note that when $d = 1$ there are no constraints and we have $N_1 = M_1$.

Proposition 3.2. *For $d > 0$, the image of the inclusion $\mathcal{R}_d \hookrightarrow M_d$ is N_d.*

Proof. For any two distinct irreducible curves C and C' we have $C \cdot C' \geq 0$. Upon taking $C \in \mathcal{R}_d$ and $C' \in \mathcal{R}_{d'}$ for $d' < d$ we see that $\mathcal{R}_d$ injects in to N_d.

Now take any $D \in N_d$. From the Riemann–Roch theorem for surfaces [40, V.1.6] we get:

$$\dim H^0(X, \mathcal{O}_X(D)) + \dim H^0(X, \mathcal{O}_X(-D)) \geq \frac{1}{2} D^2 + 2 = 1,$$

so that either D or $-D$ must be linearly equivalent to an effective divisor. Since $D \cdot h_X > 0$, $-D$ can not be so and therefore D must be.

Let us write D as a sum of classes of distinct irreducible curves $\sum_i n_i C_i$ with $n_i > 0$. Since $D^2 < 0$ there exists an index i such that $C_i \cdot D < 0$. Moreover, $C_i \cdot C_j \geq 0$ for every $j \neq i$, so $C_i^2 < 0$. By adjunction formula, we conclude that C_i is the class of a smooth rational curve [40, Ex. IV.1.8]. Furthermore, let $d' = C_i \cdot h_X$ and observe $d' \leq d$. By definition of N_d we have $d' = d$ and therefore $D = C_i$. Therefore, $\mathcal{R}_d$ surjects onto N_d. ∎

Proposition 3.2 implies that in order to compute the cardinality of the set $\mathcal{R}_d$ it suffices to compute the set N_d (see Algorithm 3.1). The latter can be easily computed from the sets $M_{d'}$

Algorithm 3.1 Finding rational curve classes on smooth quartic surfaces.

Input. The Picard group (i.e. matrix of the intersection product in some basis and the coordinates of the class of hyperplane section in the same basis) of a smooth quartic surface $X \subset \mathbb{P}^3$; an integer $d > 0$.

Output. The set $\{[C] \in \mathrm{Pic}(X) \mid C \subset X \text{ is a smooth rational curve of degree } d\}$.

function RationalCurves($\mathrm{Pic}(X)$, d)
  Compute a basis of $\mathrm{Pic}^0(X) = \{D \mid D \cdot h_X = 0\} \subset \mathrm{Pic}(X) \simeq \mathbb{Z}^\rho$
  Compute a basis of $4\,\mathrm{Pic}(X) + \mathbb{Z}h_X \subset \mathrm{Pic}(X)$
  Compute a basis of $\Lambda = \mathrm{Pic}^0(X) \cap (4\,\mathrm{Pic}(X) + \mathbb{Z}h_X) \subset \mathrm{Pic}(X)$
  $S \leftarrow \left\{D \in \Lambda \;\middle|\; -D^2 = 32 + 4d^2\right\}$ ▷ e.g. with KFP algorithm [47, 36]
  $M_d \leftarrow \left\{\frac{1}{4}(D + dh_X) \;\middle|\; D \in S\right\} \cap \mathbb{Z}^\rho$
  return $\{D \in M_d \mid \forall d' < d, \forall D' \in \text{RationalCurves}(\mathrm{Pic}(X), d'), D \cdot D' \geq 0\}$
end function

for $d' \leq d$. We now reduce the computation of M_d for each $d > 0$ to the enumeration of all vectors of a given norm in a lattice with a negative definite quadratic form.

Let $\mathrm{Pic}^0(X) = \{D \in \mathrm{Pic}(X) \mid D \cdot h_X = 0\}$. The intersection product on $\mathrm{Pic}^0(X)$ is negative definite [46, Proposition 1.2.4]. Recalling that $h_X^2 = 4$, we define a map $\pi\colon \mathrm{Pic}(X) \to \mathrm{Pic}^0(X)$ with $\pi(D) = 4D - (D \cdot h_X)h_X$.

The map π maps M_d bijectively on to the following set:

$$\overline{M}_d = \left\{E \in \mathrm{Pic}^0(X) \;\middle|\; E^2 = -(32 + 4d^2) \text{ and } E + dh_X \in 4\,\mathrm{Pic}(X)\right\}. \tag{3.2}$$

The inverse map $\overline{M}_d \to M_d$ is given by $E \mapsto \frac{1}{4}(E + dh_X)$.

In order to compute $\overline{M}_d$ we first find the finitely many elements $E \in \mathrm{Pic}^0(X)$ of norm $-(32+4d^2)$, for example using KFP algorithm [47, 36]. Then, among all such E, we select those where $\frac{1}{4}(E + dh_X)$ has integer coordinates to obtain $\overline{M}_d$. In practice, it is sufficient and more efficient to enumerate the elements of length $-(32 + 4d^2)$ in the sublattice $\pi(\mathrm{Pic}(X)) = \mathrm{Pic}^0(X) \cap (4\,\mathrm{Pic}(X) + \mathbb{Z}h_X)$.

Example 3.3. Take $f_X = 14x^4 - 85x^3z - 2xz^3 + 83y^4 - 17y^3w - 96w^4$ and let $X = Z(f_X) \subset \mathbb{P}^3$. We find that X has Picard number 18 with the following representation of $(\mathrm{Pic}(X), h_X)$:

$$\begin{bmatrix}
-4 & 0 & -1 & 0 & -1 & 2 & 0 & 0 & 0 & -2 & 0 & -2 & 0 & 1 & -1 & -1 & 0 & -2 \\
0 & -6 & -3 & -3 & -3 & 3 & 0 & -2 & -2 & -1 & 3 & -1 & -1 & 3 & -1 & 0 & 1 & 0 \\
-1 & -3 & -4 & -2 & -2 & 2 & 0 & 0 & -1 & 0 & 2 & 0 & -2 & 3 & -2 & 0 & 1 & 0 \\
0 & -3 & -2 & -4 & -2 & 2 & 1 & -1 & 0 & -1 & 1 & -1 & -1 & 2 & -1 & 0 & 1 & 0 \\
-1 & -3 & -2 & -2 & -4 & 2 & 0 & 0 & -1 & -1 & 2 & 0 & 0 & 2 & -2 & 0 & 1 & 0 \\
2 & 3 & 2 & 2 & 2 & -4 & 1 & 2 & 2 & 2 & -1 & 2 & 0 & -2 & 2 & 0 & -1 & 2 \\
0 & 0 & 0 & 1 & 0 & 1 & -4 & -2 & -2 & 1 & 1 & 1 & 0 & 0 & -1 & 2 & 1 & 1 \\
0 & -2 & 0 & -1 & 0 & 2 & -2 & -4 & -2 & 0 & 1 & -1 & 0 & 1 & 0 & 1 & 1 & 0 \\
0 & -2 & -1 & 0 & -1 & 2 & -2 & -2 & -4 & 0 & 2 & 0 & 0 & 1 & -1 & 1 & 2 & 0 \\
-2 & -1 & 0 & -1 & -1 & 2 & 1 & 0 & 0 & -4 & 0 & -2 & 1 & 0 & 0 & -2 & -1 & -2 \\
0 & 3 & 2 & 1 & 2 & -1 & 1 & 1 & 2 & 0 & -4 & 0 & 2 & -2 & 1 & -1 & -2 & -2 \\
-2 & -1 & 0 & -1 & 0 & 2 & 1 & -1 & 0 & -2 & 0 & -4 & 0 & 0 & 0 & 0 & 0 & -2 \\
0 & -1 & -2 & -1 & 0 & 0 & 0 & 0 & 0 & 1 & 2 & 0 & -4 & 3 & -1 & 1 & 2 & 2 \\
1 & 3 & 3 & 2 & 2 & -2 & 0 & 1 & 1 & 0 & -2 & 0 & 3 & -6 & 3 & 0 & -2 & 0 \\
-1 & -1 & -2 & -1 & -2 & 2 & -1 & 0 & -1 & 0 & 1 & 0 & -1 & 3 & -4 & 1 & 2 & -1 \\
-1 & 0 & 0 & 0 & 0 & 0 & 2 & 1 & 1 & -2 & -1 & 0 & 1 & 0 & 1 & -4 & -2 & -1 \\
0 & 1 & 1 & 1 & 1 & -1 & 1 & 1 & 2 & -1 & -2 & 0 & 2 & -2 & 2 & -2 & -4 & -1 \\
-2 & 0 & 0 & 0 & 0 & 2 & 1 & 0 & 0 & -2 & -2 & -2 & 2 & 0 & -1 & -1 & -1 & -4
\end{bmatrix}, \begin{bmatrix} -2 \\ -1 \\ 1 \\ 1 \\ 3 \\ 4 \\ 4 \\ 0 \\ 0 \\ 0 \\ 0 \\ 0 \\ 2 \\ 2 \\ 0 \\ -2 \\ 2 \\ -1 \\ 4 \end{bmatrix}.$$

Applying Algorithm 3.1 we see that there are 16 lines, 288 quadrics and 1536 twisted cubics as determined by this lattice of X. The 16 lines, and their incidence correspondence, as

we compute from this lattice are in agreement with what we can compute rigorously using symbolic methods.

4. Numerical reconstruction of integer relations. In view of (2.2) and (2.4), recovering $\mathrm{Pic}(X)$ boils down to finding integer linear relations between the period vectors. With the methods employed here, a finite but high enough precision will successfully recover $\mathrm{Pic}(X)$. It seems difficult to decide if a given precision is "high enough". Instead, we will study the process of finding linear relations between approximate vectors of real numbers and quantify the expected behavior of "noise", that is, of relations that are an artifact of the finite approximation (the 15th to 22nd columns in Figure 2.1). We will thus select relations whose behavior significantly differs from the expected behavior of noise.

The reconstruction of integer relations between real numbers is a well known application of the Lenstra–Lenstra–Lovász lattice basis reduction algorithm [53, p. 525], see also [13, 15]. There are many other algorithms for the problem of computing integer relations, in particular Ferguson and Forcade's algorithm [33] and the HJLS [42] and PSLQ [32, 5, 31] families. A strong point in favor of the folklore LLL approach is that efficient LLL implementations are available in most computer algebra systems.

In this section, we recall and analyze the LLL approach to solve the following problem: *Given a numerical approximation of a real matrix $P \in \mathbb{R}^{m\times p}$, with $p \leq m$, recover a basis of the lattice $\Lambda = \{x \in \mathbb{Z}^m \mid xP = 0\}$.* In our setting, the coefficients of P are the real and imaginary parts of the periods $\int_{\gamma_i} \omega_j$ of the surface X under consideration. A rigorous numerical computation of Λ faces two obstacles: the lack of an *a priori* bound on the norm of generators and the inability to recognize zero among periods. However, we can compute a candidate lattice $\tilde{\Lambda}$ that satisfy a triple alternative: either $\tilde{\Lambda} = \Lambda$; or Λ is not generated by elements of norm less that some explicit number B; or some unexpected numerical cancellation happens (Proposition 4.1).

The computation of a canditate lattice with LLL proceeds as follows. Assume that, for some large $\beta > 0$ (typically 10^{300}), we are given the exact value of the $m \times p$ integer matrix P_β obtained by entry wise rounding to the nearest integer the coefficients of βP, that is

$$P_\beta = \beta P + E, \quad \text{with } E \in [-\tfrac{1}{2}, \tfrac{1}{2}]^{p\times m}. \tag{4.1}$$

Then, we build the $m \times (p+m)$ integer matrix $M = \left[\begin{array}{c|c} P_\beta & I_m \end{array}\right]$ and compute an LLL-reduced basis $b_1, \ldots, b_m$ of the lattice spanned by the rows of M.

We complement the folklore LLL approach with the following heuristic. If β is large enough, Proposition 4.3 suggests that for $\rho = \operatorname{rk}\Lambda$ the norm $\|b_\rho\|$ is small but the norm $\|b_{\rho+1}\|$ is large and comparable to $\beta^{\frac{p}{m-\rho}}$. In this case, $\Lambda = \langle \mathrm{pr}(b_1), \ldots, \mathrm{pr}(b_\rho)\rangle$, where $\mathrm{pr}\colon \mathbb{Z}^{p+m} \to \mathbb{Z}^m$ is the projection on to the last m coordinates.

4.1. Quantitative results. For $B > 0$ and $\varepsilon > 0$ let $\Lambda_{B,\varepsilon}$ be the lattice

$$\Lambda_{B,\varepsilon} = \langle x \in \mathbb{Z}^m \mid \|x\| \leq B \text{ and } \|xP\| < \varepsilon \rangle\,. \tag{4.2}$$

For $B \geq 1$, let

$$\varepsilon(B) = \min\{\|uP\| \mid u \in \mathbb{Z}^m, \|u\| \leq B \text{ and } uP \neq 0\}\,. \tag{4.3}$$

Algorithm 4.1 Computation of the lattice of integer relations between approximate real vectors with a heuristic check.

Input. $Q \in \mathbb{Z}^{p\times m}$ and $\beta > 0$.
Precondition. $Q = \beta P + E$ for some $P \in \mathbb{R}^{p\times m}$ and $E \in [-\frac{1}{2}, \frac{1}{2}]^{p\times m}$.
Output. Fail or return a sublattice $\tilde{\Lambda} \subset \mathbb{Z}^m$ and $B, N, \varepsilon > 0$.
Postcondition. Either $\tilde{\Lambda} = \{x \in \mathbb{Z}^m \mid xP = 0\}$;
or $\{x \in \mathbb{Z}^m \mid xP = 0\}$ is not generated by vectors of norm at most B;
or $\exists x \in \mathbb{Z}^m \colon \|x\| \le N$, $\|xP\| \le \varepsilon$ and $xP \neq 0$.

function IntegerRelationLattice(Q, β)
Compute an LLL-reduced basis $b_1, \dots, b_m$ of the lattice spanned by the rows $\left[\begin{array}{c|c} Q & I_m \end{array}\right]$.
Find ρ such that $\|b_\rho\| \le 2^{-m}\|b_{\rho+1}\|$ and $\beta^{\frac{p}{m-\rho}} \approx \|b_{\rho+1}\|$. Fail if there is none.
$\tilde{\Lambda} \leftarrow \langle \mathrm{pr}(b_1), \dots, \mathrm{pr}(b_\rho)\rangle$, where $\mathrm{pr}\colon \mathbb{Z}^{p+m} \to \mathbb{Z}^m$ takes the last m coordinates.
$B \leftarrow \frac{1}{m} 2^{-\frac{m+1}{2}} \|b_{\rho+1}\|$
$N \leftarrow \|u_\rho\|$
$\varepsilon \leftarrow m\beta^{-1}N$
Return $(\tilde{\Lambda}, B, N, \varepsilon)$
end function

Equivalently, $\varepsilon(B)$ is the largest real number such that $\Lambda_{B,\varepsilon(B)} \subseteq \Lambda$. Since $\varepsilon(B)$ is non-increasing as a function of B, the quotient $B/\varepsilon(B)$ is strictly increasing as function of B. In particular, for $s \ge 0$ we may define a non-decreasing function φ with

$$\varphi(s) = \max\{B \ge 0 \mid mB/\varepsilon(B) \le s\}. \tag{4.4}$$

The growth of this function governs the ability to numerically reconstruct Λ.

As above, assume that, for some $\beta > 0$, we are given the exact value of the integer $m \times p$ matrix P_β obtained by entry wise rounding to the nearest integer the coefficients of βP. Having coefficients in $[-\frac{1}{2}, \frac{1}{2}]$, the error matrix $E = P_\beta - \beta P$ satisfies $\|E\|_{\mathrm{op}} \le \frac{1}{2}\sqrt{pm} \le m - 1$, where $\|\cdot\|_{\mathrm{op}}$ denotes the operator norm, and where we used $\frac{1}{2}\sqrt{pm} \le \frac{1}{2}m \le m - 1$, as $m \ge 2$.

Let R be the lattice generated by the rows of the integer $m \times (p + m)$ matrix $M = \left[\begin{array}{c|c} P_\beta & I_m \end{array}\right]$ and let $b_1, \dots, b_m$ be an LLL-reduced basis of R. We denote $B_0 = 0$ and $B_i = \|b_i\|$, for $1 \le i \le m$. In particular $B_0 \le B_1 \le \cdots \le B_m$. Gaps in this sequence typically separate the elements of R that come from genuine integer relations from spurious relations coming from the inaccuracy of the approximations.

Proposition 4.1. *Let $\kappa = m^{-1}2^{-\frac{m+1}{2}}$. For any $i \in \{0, \dots, m-1\}$ such that $B_i \le \kappa B_{i+1}$, at least one of the following propositions holds:*

(i) $\{\mathrm{pr}(b_1), \dots, \mathrm{pr}(b_i)\}$ *is a basis of* Λ*;*
(ii) Λ *is not generated by elements of norm* $\le \kappa B_{i+1}$*;*
(iii) $\varphi(\beta) \le B_i$*.*

Proof. By Lemma 4.2 below, we have

$$\Lambda_{B_i, m\beta^{-1}B_i} = \Lambda_{\kappa B_{i+1}, m\beta^{-1}\kappa B_{i+1}} = \langle \mathrm{pr}(b_1), \dots, \mathrm{pr}(b_i)\rangle.$$

If Λ is generated by elements of norm $\leq \kappa B_{i+1}$ then $\Lambda \subseteq \Lambda_{\kappa B_{i+1}, m\beta^{-1}\kappa B_{i+1}}$, and therefore $\Lambda \subseteq \Lambda_{B_i, m\beta^{-1}B_i}$. If moreover $\varphi(\beta) > B_i$, then $m\beta^{-1}B_i \leq \varepsilon(B_i)$, by definition of φ, and this implies that $\Lambda_{B_i, m\beta^{-1}B_i} \subseteq \Lambda$. ∎

Lemma 4.2. *For any $i \in \{0, \ldots, m-1\}$ and any $B \in [B_i, \kappa B_{i+1}]$*

$$\Lambda_{B, mB\beta^{-1}} = \langle \mathrm{pr}(b_1), \ldots, \mathrm{pr}(b_i) \rangle.$$

Proof. Let $\Lambda_i \subset \mathbb{Z}^m$ be the lattice generated by $\mathrm{pr}(b_1), \ldots, \mathrm{pr}(b_i)$ and let $R_i \subset R$ be the lattice generated by $\langle b_1, \ldots, b_i \rangle$. Let $R|_\tau$ denote the sublattice of R generated by vectors of length at most τ.

We first show $\Lambda_i \subseteq \Lambda_{B, mB\beta^{-1}}$. Let $x = \mathrm{pr}(b_j)$, with $j \leq i$. We have $\|x\| \leq \|b_j\| \leq \|b_i\| \leq B$. Moreover $b_j = \left[\begin{array}{c|c} xP_\beta & x \end{array}\right]$, so $\|xP_\beta\| < \|b_j\| \leq B$. Since $xP = \beta^{-1}(xP_\beta - xE)$, we obtain

$$\|xP\| \leq \beta^{-1} \left(\|xP_\beta\| + (m-1)\|x\| \right) < mB\beta^{-1}. \tag{4.5}$$

Conversely, let $x \in \mathbb{Z}^m$ such that $\|x\| \leq B$ and $\|xP\| < mB\beta^{-1}$. Let $r = \left[\begin{array}{c|c} xP_\beta & x \end{array}\right]$. We check that

$$\begin{aligned} \|r\| &\leq \|xP_\beta\| + \|x\| \leq \beta\|xP\| + \|xE\| + \|x\| \\ &\leq 2mB < 2^{-(m-1)/2} B_{i+1}. \end{aligned} \tag{4.6}$$

The properties of an LLL-reduced basis [60, Thm. 9] imply that no family of $i+1$ vectors in R with norms less than $2^{-(m-1)/2}B_{i+1}$ is independent. Since $b_1, \ldots, b_i$ are independent and of norm $\leq B$, it follows that $r \in \mathbb{Q}R_i$. Moreover R is a primitive lattice (that is $\mathbb{Q}R \cap \mathbb{Z}^{p+m} = R$) therefore any subset of the basis $b_1, \ldots, b_m$ of R generates a primitive lattice, so $r \in R_i$. And therefore $x = \mathrm{pr}(r) \in \Lambda_i$. ∎

The size of the gap between $B_{\mathrm{rk}\,\Lambda}$ and $B_{\mathrm{rk}\,\Lambda+1}$ can be described more precisely in terms of $\varphi(\beta)$.

Proposition 4.3. *Let $\rho = \mathrm{rk}\,\Lambda$ and let C be the smallest real number such that Λ is generated by elements of norm at most C. For any $\beta > 0$:*

(i) $B_\rho \leq \frac{1}{2}\kappa^{-1}C$;

(ii) $\varphi(\beta) \leq B_{\rho+1}$;

Moreover, if $C \leq 2\varphi(\beta)$, then

(iii) $\kappa B_{\rho+1} \leq \varphi(\beta)$;

(iv) $\mathrm{pr}(b_1), \ldots, \mathrm{pr}(b_\rho)$ *is a basis of* Λ.

Proof. For $x \in \mathbb{Z}^m$ let $r(x) = \left[\begin{array}{c|c} xP_\beta & x \end{array}\right] \in R$. If $x \in \Lambda$, that is $xP = 0$,

$$\|r(x)\| \leq \|xP_\beta\| + \|x\| \leq \beta\|xP\| + \|xE\| + \|x\| \leq m\|x\|, \tag{4.7}$$

using $P_\beta = \beta P + E$. In particular, R contains ρ independent elements of norm at most mC. This implies that $B_\rho \leq m2^{\frac{m-1}{2}}C = \frac{1}{2}\kappa^{-1}C$; this is (i).

For (ii), since Λ has rank ρ, at least one of the $\mathrm{pr}(b_1), \ldots, \mathrm{pr}(b_{\rho+1})$ is not in Λ, say $\mathrm{pr}(b_i)$, denoted x. Since $x = \mathrm{pr}(b_i) \notin \Lambda$, $xP \neq 0$ and $\|xP\| \geq \varepsilon(B_{\rho+1})$. Moreover $B_{\rho+1} \geq \|b_i\| \geq \|xP_\beta\|$, because $b_i = r(x)$. It follows

$$B_{\rho+1} \geq \beta\|xP\| - \|xE\| \geq \beta\varepsilon(B_{\rho+1}) - (m-1)B_{\rho+1}, \tag{4.8}$$

which implies $\varphi(\beta) \leq B_{\rho+1}$.

To check (iii), let $x \in \mathbb{Z}^m$ such that $\|x\| \leq \varphi(\beta)$ and $\|xP\| = \varepsilon(\varphi(\beta))$. By construction, $x \notin \Lambda$. The element $r(x) \in R$ satisfies

$$\|r(x)\| \leq \beta\|xP\| + \|xE\| + \|x\| \leq \beta\varepsilon(\varphi(\beta)) + m\varphi(\beta). \tag{4.9}$$

By definition of φ, $\beta\varepsilon(\varphi(\beta)) = m\varphi(\beta)$ and therefore $\|r(x)\| \leq 2m\varphi(\beta)$. As shown above, R contains ρ independent elements of norm $\leq mC$ that project to elements of Λ. The vector $r(x) \in R$ does not project on Λ, so R contains $\rho + 1$ independent elements of norm $\leq m\max(C, 2\varphi(\beta)) = 2\varphi(\beta)$. It follows that $\kappa B_{\rho+1} \leq \varphi(\beta)$. ∎

Minkowski's Theorem on linear forms shows that if $\varepsilon^p \beta^{m-\operatorname{rk}\Lambda-p} \geq \det(P^T P)$, there is an $x \in \Lambda^\perp \cap \mathbb{Z}^m$ such that $\|xP\| \leq p\varepsilon$. Therefore

$$\varepsilon(\beta) = O\left(\beta^{1-\frac{m-\operatorname{rk}\Lambda}{p}}\right) \quad \text{and} \quad \varphi(s) = O\left(s^{\frac{p}{m-\operatorname{rk}\Lambda}}\right). \tag{4.10}$$

We define the *irrationality measure* of P, denoted $\mu(P)$ as the infimum of all $\mu > 0$ such that $\varepsilon(\beta) = O(\beta^{1-\mu})$ as $\beta \to \infty$. As for the usual irrationality of real numbers, we can show with Borel–Cantelli Lemma that $\mu(P) = \frac{m-\operatorname{rk}\Lambda}{p}$ for almost all $P \in \mathbb{R}^{m\times p}$ with a given lattice Λ of integer relations. Generalizing Roth's Theorem on rational approximation of algebraic numbers, Schmidt [67] proved that if P has *algebraic* coefficients, with some additional hypotheses, then it again holds that $\mu(P) = \frac{m-\operatorname{rk}\Lambda}{p}$.

All in all, this leads to Algorithm 4.1. The heuristic check relies on assuming $\mu(P) = \frac{m-\operatorname{rk}\Lambda}{p}$, approximating $\varphi(\beta) \simeq \beta^{1/\mu(P)}$, that is $\varphi(\beta) \simeq \beta^{\frac{p}{m-\operatorname{rk}\Lambda}}$, and applying Proposition 4.3.

4.2. Intrinsic error bounds for the computation of the Picard group. Let $X \subset \mathbb{P}^3$ be a smooth surface of degree d, $(\gamma_i)_i$ a basis of $H_2(X, \mathbb{Z})$ and $(\omega_j)_j$ a basis of the space of holomorphic 2-forms $\Omega^2(X)$ on X. Given a numerical approximation of the period matrix $\left(\int_{\gamma_i} \omega_j\right)_{i,j}$, one can compute with Algorithm 4.1 a sublattice $\Lambda \subset H_2(X, \mathbb{Z})$ and three positive numbers B, N and ε such that one of the following hypotheses must hold:

1. $\Lambda = \operatorname{Pic}(X)$; or
2. $\operatorname{Pic}(X)$ is not generated by the set $\{\sum_i a_i\gamma_i \in \operatorname{Pic}(X) \mid \sum_i a_i^2 \leq B^2\}$; or
3. there is some $\sum_i a_i\gamma_i \in H_2(X, \mathbb{Z})$ such that

$$\sum_i a_i^2 \leq N^2 \quad \text{and} \quad 0 < \sum_j \left|\sum_i a_i \int_{\gamma_i} \omega_j\right|^2 \leq \varepsilon^2.$$

For B large enough and ε small enough the latter two possibilities can not be realized. As we have no rigorous criterion to exclude Hypotheses 2 or 3, it is important to be able to interpret them as well as possible. Currently, these conditions are not expressed in intrinsic terms and the choice of bases may affect the relevance of the triple (B, N, ε). For example, if γ_1 is replaced by $\gamma_1 + B\gamma_2$, Hypothesis 2 becomes plausible.

First, we note that $\Omega^2(X)$ is endowed with a natural Hermitian structure, defined by

$$\|\omega\|^2 \stackrel{\text{def}}{=} \int_X \omega \wedge \overline{\omega}.$$

If we choose a basis $(\omega_j)_j$ of $\Omega^2(X)$ orthonormal with respect to this Hermitian structure, then the statement of Hypothesis 3 will be independent of the choice of the orthonormal basis.

Second, following [46, Example 3.1.7(ii)], we define a canonical norm on $H_2(X,\mathbb{R})$. Let $\alpha_j, \beta_j \in H_2(X,\mathbb{R})$ be the unique homology classes such that for any $\gamma \in H_2(X,\mathbb{R})$,

$$\gamma \cdot (\alpha_j + \sqrt{-1}\beta_j) = \int_\gamma \omega_j. \tag{4.11}$$

Let U be the $\mathbb{R}$-linear subspace of $H_2(X,\mathbb{R})$ generated by h_X, α_j and β_j. Let $U^\perp$ be the orthogonal complement of U with respect to the intersection product so that $H_2(X,\mathbb{R}) = U \oplus U^\perp$. The intersection product is positive definite on U and negative definite on $U^\perp$. Therefore, the quadratic form q defined on $H_2(X,\mathbb{R})$ by

$$q(u+v) \stackrel{\text{def}}{=} u \cdot u - v \cdot v, \tag{4.12}$$

for any $u \in U$ and $v \in U^\perp$, is positive definite.

The matrix of q can be computed numerically from the intersection matrix on $H_2(X,\mathbb{R})$ and bases of U and $U^\perp$. We can compute bounds for $\sigma_{\min}(q)$ and $\sigma_{\max}(q)$, the smallest and largest eigenvalues of q respectively. For any $v = \sum_i a_i\gamma_i \in H_2(X,\mathbb{R})$, we have

$$\sigma_{\min}(q)q(v) \leq \sum_i a_i^2 \leq \sigma_{\max}(q)q(v). \tag{4.13}$$

Therefore, with $N' \stackrel{\text{def}}{=} \sigma_{\max}(q)^{1/2}N$ and $B' \stackrel{\text{def}}{=} \sigma_{\min}(q)^{1/2}B$, we obtain the following alternative hypotheses which are independent of the choice of bases:

1. $\Lambda = \mathrm{Pic}(X)$; or

2'. $\mathrm{Pic}(X)$ is not generated by the set $\{v \in \mathrm{Pic}(X) \mid q(v) \leq (B')^2\}$; or

3'. there is some $v \in H_2(X,\mathbb{Z})$ such that

$$q(v) \leq N'^2 \quad \text{and} \quad 0 < \sum_j \left| \int_v \omega_j \right|^2 \leq \varepsilon^2.$$

We obtain rigorous bounds on B', N' and ε using interval arithmetic.

Lemma 4.4 allows for another interpretation for any surface. For simplicity, let us assume X has degree four. If Hypothesis 2' fails for a surface X of degree d, then $\mathrm{Pic}(X)$ is not generated by classes of irreducible curves of degree less than B'. In our computations, B' is typically larger than 10^{100} which proves that the sublattice of $H_2(X,\mathbb{R})$ that we compute contains the classes of all irreducible algebraic curves in X of degree at most 10^{100}. In particular, our count of smooth rational curves (up to degree 10^{100}) gives rigorous upper bounds for the correct numbers.

Lemma 4.4. *If X is a smooth surface of degree d and $D \in \mathrm{Pic}(X)$ the class of an irreducible curve of degree δ, then $q(D) \leq 2 + (d-4)\delta + \frac{2}{d}\delta^2$.*

Proof. Any $D \in \mathrm{Pic}(X)$ decomposes as

$$D = \tfrac{1}{d}(D \cdot h_X)h_X + \left(D - \tfrac{1}{d}(D \cdot h_X)h_X\right),$$

with the first and second terms respectively in U and $U^\perp$. Therefore

$$\begin{aligned} q(D) &= \tfrac{1}{d^2}(D \cdot h_X)^2(h_X \cdot h_X) - \big(D - \tfrac{1}{d}(D \cdot h_X)h_X\big)^2 \\ &= -D^2 + \tfrac{2}{d}(D \cdot h_X)^2. \end{aligned}$$

In particular, if D is the class of an irreducible curve $C \subset X$ of degree δ and arithmetic genus p_a, then $-D \cdot (D + K_X) = 2 - 2p_a \leq 2$ and $D \cdot h_X = \delta$. Moreover $K_X = (d-4)h_X$ [40, Ex. 8.20.3], therefore

$$\begin{aligned} q(D) &= -D \cdot (D + K_X) + (d-4)D \cdot h_X + \tfrac{2}{d}(D \cdot h_X)^2 \\ &\leq 2 + (d-4)\delta + \tfrac{2}{d}\delta^2. \end{aligned}$$

■

5. Hypersurfaces of arbitrary even dimension. Let k be a positive integer and let $X \subset \mathbb{P}^{2k+1}$ be a smooth hypersurface. Using Lefschetz hyperplane theorem and Poincaré duality we see that the cohomology groups $H^i(X, \mathbb{Z})$ are either trivial or $\mathbb{Z}$ except when $i = 2k$. The Hodge decomposition on de Rham cohomology gives

$$H^{2k}_{\mathrm{dR}}(X, \mathbb{C}) = \bigoplus_{p+q=2k} H^{p,q}(X, \mathbb{C}). \tag{5.1}$$

Algebraic cycles of dimension k in X give cohomology classes in

$$\mathrm{Hdg}^k(X) \stackrel{\mathrm{def}}{=} H^{k,k}(X, \mathbb{C}) \cap H^{2k}(X, \mathbb{Z}). \tag{5.2}$$

As a generalization of Theorem 2.1, the Hodge conjecture predicts that the vector space $\mathrm{Hdg}^k(X) \otimes_{\mathbb{Z}} \mathbb{Q}$ is spanned by algebraic cycles [81].

The Hodge group $\mathrm{Hdg}^k(X)$ comes with an intersection pairing obtained by restricting the cup product on cohomology $H^{2k}(X, \mathbb{C})$. Furthermore, there is a *polarization* $h_X^k \in \mathrm{Hdg}^k(X)$ where h_X is the class of a generic hyperplane section of X. The tools we used to tackle the computation of Picard groups apply to the following problem: *given the defining equation of* $X \subset \mathbb{P}^{2k+1}$*, compute the rank* ρ *of* $\mathrm{Hdg}^k(X)$*, the* $\rho \times \rho$ *matrix of the intersection product and the* ρ *coordinates of the polarization* h_X^k *in some basis of* $\mathrm{Hdg}^k(X) \simeq \mathbb{Z}^\rho$*.*

Suppose now that $\gamma_1, \ldots, \gamma_m \in H_{2k}(X, \mathbb{Z})$ is a basis for the middle homology group of X. We can then identify the cohomology $H^{2k}(X, \mathbb{C}) = \mathrm{Hom}(H_{2k}(X, \mathbb{Z}), \mathbb{C})$ with $\mathbb{C}^m$ via the dual basis of $\{\gamma_i\}_{i=1}^m$. Let us write $F^{2k,\ell}(X, \mathbb{C}) = \bigoplus_{j=0}^{\ell} H^{2k-j,j}(X, \mathbb{C})$ for the corresponding Hodge filtration.

Let $\omega_1, \ldots, \omega_s \in F^{2k,k-1}(X, \mathbb{C})$ be a basis for the $(k-1)$-th part of the Hodge filtration. Suppose that we have the coordinates of ω_i with respect to the identification $H^n(X, \mathbb{C}) \simeq \mathbb{C}^m$, that is, suppose that for each $i = 1, \ldots, s$ the following integrals are known

$$\left(\int_{\gamma_1} \omega_i, \ldots, \int_{\gamma_m} \omega_i \right) \in \mathbb{C}^m. \tag{5.3}$$

These *periods* of X are listed as the columns of the following matrix:

$$\mathcal{P} \stackrel{\mathrm{def}}{=} \left(\int_{\gamma_i} \omega_j \right)_{\substack{i=1,\ldots,m \\ j=1,\ldots,s}}. \tag{5.4}$$

The matrix $\mathcal{P}$ induces the linear map $\mathcal{P}_{\mathbb{Z}}\colon \mathbb{Z}^m \to \mathbb{C}^s$ by acting on the integral vectors from the right.

Lemma 5.1. *We have a natural isomorphism* $\mathrm{Hdg}^k(X) \simeq \ker \mathcal{P}_{\mathbb{Z}}$.

Proof. The kernel of $\mathcal{P}_{\mathbb{Z}}$ computes in $H_{2k}(X,\mathbb{Z})$ the classes annihilated by $F^{2k,k-1}(X,\mathbb{C})$. Any integral (or real) class annihilated by $F^{2k,k-1}$ will also be annihilated by its complex conjugate $\overline{F^{2k,k-1}}$. We now use the equality $H^{k,k}(X,\mathbb{C}) = \left(F^{2k,k-1} \oplus \overline{F^{2k,k-1}}\right)^{\perp}$ and the definition of Poincaré duality. ∎

The kernel of $\mathcal{P}_{\mathbb{Z}}$ sits most naturally in homology $H_{2k}(X,\mathbb{Z})$ and is denoted by $\mathrm{Hdg}_k(X)$. We can approximate the matrix $\mathcal{P}$ to the desired degree of accuracy for an automatically generated basis of $F^{2k,k-1}(X,\mathbb{C})$ and some implicit basis of $H_{2k}(X,\mathbb{Z})$ [68]. The basis of $H_{2k}(X,\mathbb{Z})$ comes with an intersection pairing as well as the coordinates of the polarization h_X^k in this basis.

In light of Lemma 5.1, it remains to compute integral linear relations between the columns of $\mathcal{P}$ to recover $\mathrm{Hdg}_k(X)$. That is the problem studied in §4.

The study of the Hodge groups of cubic fourfolds is an active area of research [66, 3]. Although generic cubic fourfolds provide a computational challenge, we can quickly compute the Hodge rank of sparse cubic fourfolds if most of the monomial terms are cubes of a single variable.

Example 5.2. Let X be the cubic fourfold in $\mathbb{P}^5$ cut out by the equation

$$6x_0^3 + 10x_0x_2x_4 + 9x_0x_2x_5 + 4x_1^3 + 2x_1x_2^2 + 4x_2^3 + 3x_3^3 + 4x_4^3 + 9x_5^3. \tag{5.5}$$

We find that $\mathrm{Hdg}^2(X)$ is of rank 13.

6. Experimental results. We put our methods into practice and computed the Picard lattices of thousands of smooth quartic surfaces defined by sparse polynomials. For these computations, setting up the initial value problem for the periods was not the limiting factor but rather the numerical solution of these initial value problems took the greatest amount of time. With our current methods, the periods of a quartic surface defined by dense polynomials may take weeks to compute. Further work will address the problem.

As a first experiment, we performed a systematic exploration of quartics that are defined by a sum of at most six monomials in x, y, z, w with coefficients 0 or 1. We built a graph whose vertices store the defining polynomials and an edge between two polynomial is constructed if the difference of the two polynomials is supported on at most two monomials (this is done to ease the computations). Then, for each edge, we setup and attempt to solve the initial value problem defining the transition matrix from one set of periods onto the other, using 300 decimal digits of precision, see [68] for details. Computation is stopped if it takes longer than an hour and the edge deleted. Having explicit formulas for the periods of Fermat surface $\{x^4 + y^4 + z^4 + w^4 = 0\}$, we can compute the periods of any vertex in the connected component of $x^4 + y^4 + z^4 + w^4$ in the resulting graph by simply multiplying the transition matrices of each edge along a path.

For each of the 2790 polynomials in this graph, we computed the Picard group, the polarization, the intersection product, the endomorphism ring and the number of smooth

Defining polynomial	Picard number
$wx^3 + w^3y + y^4 + xz^3 + z^4$	1
$x^3y + z^4 + y^3w + zw^3$	4
$x^3y + y^4 + z^3w + yw^3 + zw^3$	6
$w^3x + x^4 + wx^2z + x^3z + xy^2z - y^3z + wxz^2 + x^2z^2 - xz^3 + z^4$	7
$x^3y + z^4 + y^3w + xw^3 + w^4$	8
$w^4 + wx^2y + y^4 + x^3z - xy^2z + z^4$	9
$x^3y + z^4 + y^3w + w^4$	10
$w^4 + x^4 + x^2y^2 + y^4 - w^3z - {}^2\, xy^2z + x^2z^2 + z^4$	11
$x^3y + y^4 + z^3w + x^2w^2 + w^4$	12
$w^4 + {}^3\, x^4 + wy^3 + y^2z^2 + wz^3 + {}^2\, xz^3$	13
$x^3y + y^4 + z^3w + yw^3 + w^4$	14
$x^3y + y^3z + z^4 + xy^2w + zw^3$	15
$x^3y + y^4 + z^3w + xyw^2 + y^2w^2 + w^4$	16
$x^3y + y^4 + z^4 + x^2w^2 + zw^3$	17
$x^3y + x^3z + y^3z + yz^3 + w^4$	18
$x^3y + z^4 + y^3w + xyzw + xw^3$	19
$x^3y + z^4 + y^3w + xw^3$	20

Figure 6.1. *Specimen polynomials for each Picard number found*

rational curves of degree up to 4. We found quartic surfaces with Picard number 4, 6, 8, 10, 12, 14, 15, 16, 17, 18, 19 and 20, see Figures 6.1 and 6.2. When possible, we checked that our results were consistent with Shioda's formula for 4-nomial quartic surfaces [69], reduction methods with Costa's implementation [19] and symbolic line counting.

Afterwards, we extended our collection of quartics by following a random walk in the space of homogeneous polynomials of degree 4 in 4 variables, where each step adds or substracts a monomial. We computed the periods of more than 180,000 quartics as well as the related data: Picard lattice, endomorphism ring of the transcendental lattice, number of smooth rational curves of degree at most 4.[8]

We give a few interesting examples below. Of course, all the assertions were obtained through numerical computations, so they are not proved.

Example 6.1. $\{x^4 + y^3z + xyzw + z^3w + yw^3 = 0\}$. This surface has Picard number 19. It contains no smooth rational curves of degree < 4 but has 133056 smooth rational curves of degree 4. These generate the Picard group.

Example 6.2. $\{x^3y + x^3z + y^3z + yz^3 + z^4 + xw^3 = 0\}$. This surface has Picard number 10. It contains 13 lines that generate the Picard group. The endomorphism ring is $\mathbb{Q}(\exp(\frac{2\pi i}{18}))$, a cyclotomic extension of $\mathbb{Q}$ of degree 6. Up to degree 10, the number of smooth rational curves inside X are as follows.

[8] Results are compiled at https://pierre.lairez.fr/quarticdb.

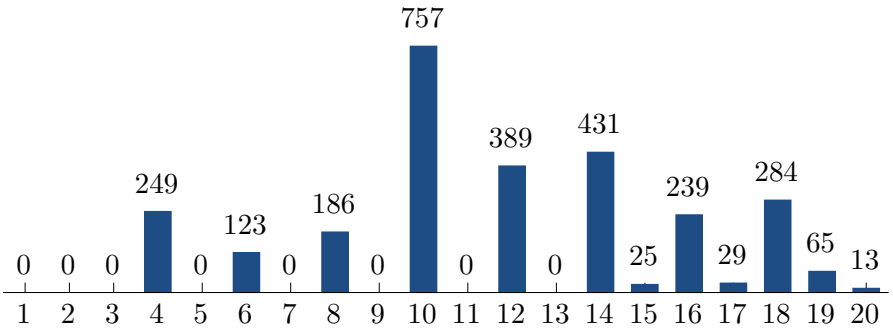

Figure 6.2. *Occurence of Picard numbers in the graph of 4-nomials and 5-nomials*

d	1	2	3	4	5	6	7	8	9	10
$\#\mathcal{R}_d$	13	0	0	108	0	0	972	0	0	3996

Example 6.3. $\{x^3y + z^4 + y^3w + zw^3 = 0\}$. This surface has Picard number 4. It contains exactly 4 lines that generate the Picard group and no other smooth rational curve of degree < 100. The endomorphism ring is $\mathbb{Q}(\exp(\frac{\pi i}{27}))$, a cyclotomic extension of $\mathbb{Q}$ of degree 18. They actually all come from the diagonal morphism

$$(x, y, z, w) \mapsto (\zeta^9 w, \zeta x, \zeta^{-3} y, \zeta^{-27} z),$$

for some primitive 108th root of unity ζ, that fixes the defining polynomial of the surface.

Example 6.4. $\{w^4+x^4+xy^3+y^4+w^3z+xyz^2+z^4 = 0\}$. This surface has Picard number 9. It contains no smooth rational curves of degree ≤ 21 (the space complexity of the search makes it difficult to search for higher degree curves). The Picard lattice is generated by smooth quartic curves of genus 1. It would be interesting to settle the existence of rational curves on this surface.

Example 6.5. $\{wx^3 + w^3y + y^4 + xz^3 + z^4 = 0\}$. This surface has Picard number 1. The first example of such a quartic surface defined over $\mathbb{Q}$ was given recently by van Luijk [78]. As Picard number 1 is the smallest possible value, implementations of finite characteristic methods, e.g. *controlledreduction* [19], can readily prove that this is the correct number.

7. Computing the coordinates of the polarization. Let $X = Z(f_X) \subset \mathbb{P}^{n+1}$ be a smooth hypersurface of degree d and assume n is even. We compute a basis for the middle integral homology $H_n(X, \mathbb{Z})$ by carrying over a basis from a hypersurface of Fermat type [68, §1.3]. If $h_X = [X \cap H]$ denotes the hyperplane class in X, then $h_X^{n/2} \in H_n(X, \mathbb{Z})$ is the polarization. The orthogonal complement of $h_X^{n/2}$ is the *primitive homology*, denoted $PH_n(X, \mathbb{Z})$. In order to compute the periods of X, it is sufficient to work only with the primitive homology $PH_n(X, \mathbb{Z})$ as is done in [68]. In §4.5 of *loc. cit.* there is a sketch on how to complete the given basis for the primitive homology to a basis of homology. In this section we flesh out the details as the particular choices we make in completing the basis determine the coordinates of the

polarization. The problem that must be addressed is that $h_X^{n/2}$ and $PH_n(X,\mathbb{Z})$ do not generate $H_n(X,\mathbb{Z})$ but a full rank sublattice.

In [68] the Fermat surface $Y = Z(x_0^d + \cdots + x_n^d - x_{n+1}^d)$ was used for the construction of a basis of primitive homology. This basis is formed using a *Pham cycle* and the Pham cycle itself is formed by gluing translates of the following simplex:

$$D = \{[s_0 : s_1 : \cdots : s_n : 1] \mid s_i \in [0,1],\ s_0^d + \cdots + s_n^d = 1\} \subset Y.$$

For $\beta = (\beta_0, \ldots, \beta_{n+1}) \in \mathbb{Z}^{n+2}$ we define the translations $t^\beta \colon \mathbb{P}^{n+1} \to \mathbb{P}^{n+1}$ by the action on the coordinates $x_i \mapsto \xi^{\beta_i} x^i$. Then the Pham cycle S is defined by:

$$S = (1 - t_0^{-1}) \cdots (1 - t_n^{-1}) D,$$

where summation is union and negation is change of orientation [63]. It is possible to compute a subset $B \subset \mathbb{Z}^{n+2}$ for which the set $\{t^\beta S\}_{\beta \in B}$ is a basis for the primitive homology $PH_n(Y,\mathbb{Z})$, for instance, use Corollary 4.8 [68]. We will now add one more cycle to complete $\{t^\beta S\}_{\beta \in B}$ to a basis of homology.

With d being the degree of X and Y, we denote the d-th root of -1 by $\eta := \exp(\frac{\pi\sqrt{-1}}{d})$ and the d-th root of 1 by $\xi := \exp(\frac{2\pi\sqrt{-1}}{d})$. Let $\mathbb{P}^{n/2}$ be a projective space with coordinate functions $\mu_0, \ldots, \mu_{n/2}$ and consider the linear map $\mathbb{P}^{n/2} \to \mathbb{P}^{n+1}$ defined by

$$\begin{aligned} x_{2k} = \mu_k,\ x_{2k+1} = \eta\mu_k \quad k = 0, \ldots, \frac{n}{2} - 1, \\ x_n = \mu_{\frac{n}{2}},\ x_{n+1} = \mu_{\frac{n}{2}}. \end{aligned} \tag{7.1}$$

The image of this map is a linear space L which is evidently contained in Y. Let $[L]$ be the homology class of L and let γ_β be the homology class of $t^\beta S$. The set $\{[L]\} \cup \{\gamma_\beta\}_{\beta \in B}$ is a basis for the integral homology $H_n(X,\mathbb{Z})$.

As Y is deformed into X, the homology class of L will typically deform into a class which no longer supports an algebraic subvariety and therefore this class will typically have non-zero periods. Nevertheless, we can deduce the periods of L as it deforms based on the following two observations: The polarization $h_Y^{n/2}$ deforms in to $h_X^{n/2}$ and will always remain algebraic throughout the deformation. We will know the periods of the Pham basis $\{t^\beta S\}_{\beta \in B}$ as it deforms.

The homology with rational coefficients $H_n(Y,\mathbb{Q})$ splits into the direct sum $PH_n(Y,\mathbb{Q}) \oplus \mathbb{Q}\langle h_Y^{n/2} \rangle$ so that we may write:

$$[L] = \frac{1}{d} h_Y^{\frac{n}{2}} + \sum_{\beta \in B} a_\beta \gamma_\beta. \tag{7.2}$$

The coefficients $\{a_\beta\}_{\beta \in B} \subset \mathbb{Q}$ of this relation remain constant as we carry the basis $\{[L]\} \cup \{\gamma_\beta\}_{\beta \in B}$ to a basis of $H_n(X,\mathbb{Z})$. The problem of computing the periods of L as it deforms is therefore reduced to computing the coefficients $\{a_\beta\}_{\beta \in B}$. Put an ordering on B and let

$$a_{B,L} = (a_\beta)_{\beta \in B} \in \mathbb{Q}^{\#B} \tag{7.3}$$

denote the row vector of coefficients defined in (7.2).

Let $b_{B,L} = ([L] \cdot \gamma_\beta)_{\beta \in B} \in \mathbb{Q}^{\#B}$ be the intersection numbers of L with the Pham basis and let $M_B = (\gamma_\beta \cdot \gamma_{\beta'})_{\beta,\beta' \in B}$ be the matrix of intersections of the Pham basis. We see that $a_{B,L} = M_B^{-1} b_{B,L}$ so it remains to compute M_B and $b_{B,L}$.

Fix $d \geq 2$ and define a function $\chi \colon \mathbb{Z} \to \{-1, 0, 1\}$ as follows:

$$\chi(b) = \begin{cases} 1 & \text{if } b = 0 \mod d \\ -1 & \text{if } b \equiv 1 \mod d \\ 0 & \text{if } b \not\equiv 0, 1 \mod d. \end{cases}$$

Proposition 7.1. *For $\beta = (\beta_i)_{i=0}^{n+1}, \beta' = (\beta'_i)_{i=0}^{n+1} \in \mathbb{Z}^{n+2}$ let $\beta'' = (\beta_i - \beta'_i - \beta_{n+1} + \beta'_{n+1})_{i=0}^{n+1}$. The Pham cycles $t^\beta S$ and $t^{\beta'} S$ intersect as follows:*

$$\langle t^\beta S, t^{\beta'} S \rangle = (-1)^{\frac{(n+1)n}{2}} \left(\prod_{i=0}^{n} \chi(\beta''_i) - \prod_{i=0}^{n} \chi(\beta''_i + 1) \right).$$

For a proof of Proposition 7.1 see any one of [4, 58, 55]. We reformulated the statement here for the choices that were made in [68] and in the style that was first communicated to us by Degtyarev and Shimada.

Define the function $\tau_d : \mathbb{Z} \to \{-1, 0, 1\}$ where:

$$\tau_d(i) = \begin{cases} 1 & i \equiv 1 \pmod{2d} \\ -1 & i \equiv -1 \pmod{2d} \\ 0 & \text{otherwise.} \end{cases}$$

Lemma 7.2. *The intersection pairing of the linear space L with the translates of the Pham cycle S can be expressed as follows:*

$$\langle L, t^\beta S \rangle = \tau_d(2\beta_n - 2\beta_{n+1} - 1) \prod_{i=0}^{\frac{n}{2}-1} \tau_d(2\beta_{2i} - 2\beta_{2i+1} + 1).$$

Lemma 7.2 is proven by a straightforward application of Theorem 2.2 in [23].

Example 7.3. Let us consider quartic surfaces in $\mathbb{P}^3$, that is $d = 4$ and $n = 2$. Using Corollary 4.8 [68] we find

$$\begin{aligned} B = \{&(0,0,0,0), (0,0,1,0), (0,1,0,0), (1,0,0,0), (0,0,2,0), (0,1,1,0), (1,0,1,0), \\ &(0,2,0,0), (1,1,0,0), (2,0,0,0), (0,1,2,0), (1,0,2,0), (0,2,1,0), (1,1,1,0), \\ &(2,0,1,0), (1,2,0,0), (2,1,0,0), (0,2,2,0), (1,1,2,0), (2,0,2,0), (1,2,1,0)\}. \end{aligned}$$

With respect to this basis, and the ordering presented above, we find that the vector $a_{B,L}$ of (7.3) is given by

$$a_{B,L} = (0, -1, \tfrac{1}{2}, 0, 0, \tfrac{1}{2}, -1, 0, \tfrac{1}{2}, 0, \tfrac{3}{4}, \tfrac{1}{4}, -\tfrac{1}{4}, -\tfrac{1}{2}, -\tfrac{1}{4}, -\tfrac{3}{4}, \tfrac{1}{4}, 0, 0, \tfrac{1}{2}, -\tfrac{1}{2}). \tag{7.4}$$

The set $\{\gamma_\beta\}_{\beta \in B}$ is completed to a basis with the addition of $[L]$. In this basis, Equation (7.2) gives us the coordinates of the polarization:

$$h_X = (0, 4, -2, 0, 0, -2, 4, 0, -2, 0, -3, -1, 1, 2, 1, 3, -1, 0, 0, -2, 2, 4). \tag{7.5}$$

REFERENCES

[1] *Elliptic curves, modular forms and cryptography*, Proceedings of the Advanced Instructional Workshop on Algebraic Number Theory, Hindustan Book Agency, New Delhi, 2003.

[2] T. G. Abbott, K. S. Kedlaya, and D. Roe, *Bounding picard numbers of surfaces using p-adic cohomology*, in Arithmetics, geometry, and coding theory (AGCT 2005), vol. 21 of Sémin. Congr., Soc. Math. France, Paris, 2010, p. 125–159.

[3] N. Addington and A. Auel, *Some non-special cubic fourfolds*, https://arxiv.org/abs/1703.05923.

[4] V. I. Arnold, S. M. Gusein-Zade, and A. N. Varchenko, *Singularities of differentiable maps. Volume 2*, Monographs in mathematics; vol. 82, Birkhäuser, 1988.

[5] D. Bailey, *Integer relation detection*, Comput. Sci. Eng., 2 (2008), pp. 24–48, https://doi.org/10.1109/5992.814653.

[6] W. Barth, K. Hulek, C. Peters, and A. van de Ven, *Compact Complex Surfaces*, A Series of Modern Surveys in Mathematics, Springer-Verlag, Berlin Heidelberg, 2 ed., 2004.

[7] A. R. Booker, J. Sijsling, A. V. Sutherland, J. Voight, and D. Yasaki, *A database of genus-2 curves over the rational numbers*, LMS J. Comput. Math., 19 (2016), pp. 235–254, https://doi.org/10.1112/S146115701600019X.

[8] W. Bosma, J. Cannon, and C. Playoust, *The Magma algebra system. I. The user language*, J. Symbolic Comput., 24 (1997), pp. 235–265, https://doi.org/10.1006/jsco.1996.0125. Computational algebra and number theory (London, 1993).

[9] A. Bostan, P. Lairez, and B. Salvy, *Creative telescoping for rational functions using the Griffiths–Dwork method*, in Proceedings of the 38th International Symposium on Symbolic and Algebraic Computation, New York, NY, USA, 2013, ACM, pp. 93–100, https://doi.org/10.1145/2465506.2465935. ISSAC 2013 (Boston).

[10] D. J. Broadhurst and D. Kreimer, *Knots and numbers in φ^4 theory to 7 loops and beyond*, Internat. J. Modern Phys. C, 6 (1995), p. 519–524, https://doi.org/10.1142/S012918319500037X.

[11] F. Brown, *Mixed tate motives over $\mathbb{Z}$*, Ann. of Math. (2), 175 (2012), p. 949–976, https://doi.org/10.4007/annals.2012.175.2.10.

[12] N. Bruin, J. Sijsling, and A. Zotine, *Numerical computation of endomorphism rings of Jacobians*, Open Book Ser., 2 (2019), pp. 155–171, https://doi.org/10.2140/obs.2019.2.155. 13th Algorithmic Number Theory Symposium.

[13] J. Buchmann and M. Pohst, *Computing a lattice basis from a system of generating vectors*, in Eurocal '87, J. H. Davenport, ed., vol. 378 of Lecture Notes in Computer Science, Springer Berlin Heidelberg, 1989, pp. 54–63.

[14] F. Charles, *On the Picard number of K3 surfaces over number fields*, Algebra Number Theory, 8 (2014), pp. 1–17, https://doi.org/10.2140/ant.2014.8.1.

[15] J. Chen, D. Stehlé, and G. Villard, *A New View on HJLS and PSLQ: Sums and Projections of Lattices*, in Proceedings of the 38th International Symposium on Symbolic and Algebraic Computation, ISSAC '13, New York, NY, USA, 2013, ACM, pp. 149–156, https://doi.org/10.1145/2465506.2465936.

[16] D. V. Chudnovsky and G. V. Chudnovsky, *Computer algebra in the service of mathematical physics and number theory*, in Computers in Mathematics (Stanford, CA, 1986), vol. 125 of Lecture Notes in Pure and Appl. Math., Dekker, New York, 1990, pp. 109–232.

[17] F. Chyzak, *An extension of Zeilberger's fast algorithm to general holonomic functions*, Discrete Math., 217 (2000), pp. 115–134, https://doi.org/10.1016/S0012-365X(99)00259-9. Formal power series and algebraic combinatorics (Vienna, 1997).

[18] C. Ciliberto, J. Harris, and R. Miranda, *General components of the Noether-Lefschetz locus and their density in the space of all surfaces*, Math. Ann., 282 (1988), pp. 667–680.

[19] E. Costa, *Effective computations of Hasse–Weil zeta functions*, ProQuest LLC, Ann Arbor, MI, 2015. Thesis (Ph.D.)–New York University.

[20] E. Costa, D. Harvey, and K. S. Kedlaya, *Zeta functions of nondegenerate hypersurfaces in toric varieties via controlled reduction in p-adic cohomology*. 2018, https://arxiv.org/abs/1806.00368.

[21] E. Costa, N. Mascot, J. Sijsling, and J. Voight, *Rigorous computation of the endomorphism ring of a Jacobian*, Math. Comp., 88 (2019), pp. 1303–1339.

[22] B. Deconinck and M. S. Patterson, *Computing with Plane Algebraic Curves and Riemann Surfaces:*

The Algorithms of the Maple Package "Algcurves", Springer Berlin Heidelberg, Berlin, Heidelberg, 2011, pp. 67–123.

[23] A. Degtyarev and I. Shimada, *On the topology of projective subspaces in complex Fermat varieties*, J. Math. Soc. Japan, 68 (2016), pp. 975–996.

[24] P. Deligne, *The Hodge conjecture*, in The millennium prize problems, Clay Math. Inst., Cambridge, MA, 2006, pp. 45–53.

[25] S. Di Rocco, D. Eklund, C. Peterson, and A. J. Sommese, *Chern numbers of smooth varieties via homotopy continuation and intersection theory*, J. Symb. Comput., 46 (2011), pp. 23–33, https://doi.org/10.1016/j.jsc.2010.06.026.

[26] I. V. Dolgachev, *Mirror symmetry for lattice polarized K3 surfaces*, J. Math. Sci., 81 (1996), pp. 2599–2630, https://doi.org/10.1007/BF02362332.

[27] I. V. Dolgachev, *Luigi Cremona and cubic surfaces*, in Luigi Cremona (1830–1903) (Italian), vol. 36 of Incontr. Studio, Istituto Lombardo di Scienze e Lettere, Milan, 2005, pp. 55–70.

[28] A.-S. Elsenhans and J. Jahnel, *On the computation of the Picard group for K3 surfaces*, Math. Proc. Camb. Philos. Soc., 151 (2011), pp. 263–270, https://doi.org/10.1017/S0305004111000326.

[29] A.-S. Elsenhans and J. Jahnel, *The picard group of a k3 surface and its reduction modulo p*, Algebra Number Theory, 5 (2011), pp. 1027–1040, https://doi.org/10.2140/ant.2011.5.1027.

[30] A.-S. Elsenhans and J. Jahnel, *Kummer surfaces and the computation of the Picard group*, LMS J. Comput. Math., 15 (2012), pp. 84–100.

[31] Y. Feng, J. Chen, and W. Wu, *The PSLQ algorithm for empirical data*, Math. Comp., (2018), https://doi.org/10.1090/mcom/3356.

[32] H. R. P. Ferguson, D. H. Bailey, and S. Arno, *Analysis of PSLQ, an integer relation finding algorithm*, Math. Comput., 68 (1999), pp. 351–370, https://doi.org/10.1090/S0025-5718-99-00995-3.

[33] H. R. P. Ferguson and R. W. Forcade, *Generalization of the Euclidean algorithm for real numbers to all dimensions higher than two*, Bull. Am. Math. Soc., 1 (1979), pp. 912–915, https://doi.org/10.1090/S0273-0979-1979-14691-3.

[34] D. Festi, *A practical algorithm to compute the geometric Picard lattice of K3 surfaces of degree 2*, Aug. 2018, https://arxiv.org/abs/1808.00351.

[35] D. Festi and D. van Straten, *Bhabha scattering and a special pencil of K3 surfaces*, https://arxiv.org/abs/1809.04970.

[36] U. Fincke and M. Pohst, *A procedure for determining algebraic integers of given norm*, in Computer Algebra, J. A. van Hulzen, ed., Lecture Notes in Computer Science, Springer Berlin Heidelberg, 1983, pp. 194–202.

[37] F. Gesztesy and H. Holden, *Soliton equations and their algebro-geometric solutions. Vol. I*, vol. 79 of Cambridge Studies in Advanced Mathematics, Cambridge University Press, Cambridge, 2003. $(1+1)$-dimensional continuous models.

[38] P. A. Griffiths, *On the periods of certain rational integrals. I, II*, Ann. of Math. (2) 90 (1969), 460-495; ibid. (2), 90 (1969), pp. 496–541.

[39] P. A. Griffiths, *A transcendental method in algebraic geometry*, in Actes Du Congrès International Des Mathématiciens (Nice, 1970), Tome 1, Gauthier-Villars, Paris, 1971, pp. 113–119.

[40] R. Hartshorne, *Algebraic Geometry*, Springer-Verlag, New York, 1977. Graduate Texts in Mathematics, No. 52.

[41] B. Hassett, A. Kresch, and Y. Tschinkel, *Effective computation of Picard groups and Brauer-Manin obstructions of degree two K3 surfaces over number fields*, Rendiconti Circolo Mat. Palermo, 62 (2013), pp. 137–151, https://doi.org/10.1007/s12215-013-0116-8.

[42] J. Hastad, B. Just, J. C. Lagarias, and C. P. Schnorr, *Polynomial time algorithms for finding integer relations among real numbers*, SIAM J. Comput., 18 (1989), pp. 859–881.

[43] J. D. Hauenstein, J. I. Rodriguez, and F. Sottile, *Numerical Computation of Galois Groups*, Found Comput Math, (2017), pp. 1–24, https://doi.org/10.1007/s10208-017-9356-x.

[44] K. Hori, S. Katz, A. Klemm, R. Pandharipande, R. Thomas, C. Vafa, R. Vakil, and E. Zaslow, *Mirror symmetry*, vol. 1 of Clay Mathematics Monographs, American Mathematical Society, Providence, RI; Clay Mathematics Institute, Cambridge, MA, 2003. With a preface by Vafa.

[45] C. Houzel, *La Géométrie Algébrique*, Librairie Scientifique et Technique, Albert Blanchard, Paris, 2002.

[46] D. Huybrechts, *Lectures on K3 surfaces*, vol. 158 of Cambridge Studies in Advanced Mathematics,

Cambridge University Press, Cambridge, 2016.
[47] R. Kannan, *Improved algorithms for integer programming and related lattice problems*, in Proceedings of the Fifteenth Annual ACM Symposium on Theory of Computing, STOC '83, New York, NY, USA, 1983, ACM, pp. 193–206, https://doi.org/10.1145/800061.808749.
[48] K. S. Kedlaya, *Computing zeta functions via p-adic cohomology*, in Algorithmic number theory, vol. 3076 of Lecture Notes in Comput. Sci., Springer, Berlin, 2004, pp. 1–17.
[49] C. Koutschan, *A fast approach to creative telescoping*, Math. Comput. Sci., 4 (2010), pp. 259–266, https://doi.org/10.1007/s11786-010-0055-0.
[50] P. Lairez, *Computing periods of rational integrals*, Math. Comput., 85 (2016), pp. 1719–1752, https://doi.org/10.1090/mcom/3054.
[51] A. G. B. Lauder, *Counting solutions to equations in many variables over finite fields*, Found. Comput. Math., 4 (2004), pp. 221–267.
[52] S. Lefschetz, *L'analysis situs et la géométrie algébrique*, Gauthier-Villars, Paris, 1950.
[53] A. K. Lenstra, H. W. Lenstra, and L. Lovàsz, *Factoring polynomials with rational coefficients*, Math. Ann., 261 (1982), pp. 515–534, https://doi.org/10.1007/BF01457454.
[54] D. Lombardo, *Computing the geometric endomorphism ring of a genus-2 Jacobian*, Math. Comp., 88 (2019), pp. 889–929.
[55] E. Looijenga, *Fermat varieties and the periods of some hypersurfaces*, in Algebraic and arithmetic structures of moduli spaces (Sapporo 2007), vol. 58 of Adv. Stud. Pure Math., Math. Soc. Japan, Tokyo, 2010, pp. 47–67.
[56] M. Mezzarobba, *NumGFun: A package for numerical and analytic computation with D-finite functions*, in Proceedings of the 35th International Symposium on Symbolic and Algebraic Computation, S. M. Watt, ed., ACM, 2010, pp. 139–146, https://doi.org/10.1145/1837934.1837965. ISSAC 2010 (Munich).
[57] M. Mezzarobba, *Rigorous multiple-precision evaluation of D-finite functions in Sagemath*, 2016, https://arxiv.org/abs/1607.01967.
[58] H. Movasati, *A course in Hodge theory, with emphasis in multiple integrals*. to appear, w3.impa.br/~hossein/myarticles/hodgetheory.pdf.
[59] H. Movasati, *Calculation of mixed Hodge structures, Gauss-Manin connections and Picard-Fuchs equations*, in Real and Complex Singularities, Trends Math., Birkhäuser, Basel, 2007, pp. 247–262.
[60] P. Q. Nguyen, *Hermite's Constant and Lattice Algorithms*, in The LLL Algorithm, P. Q. Nguyen and B. Vallée, eds., Springer Berlin Heidelberg, Berlin, Heidelberg, 2009, pp. 19–69, https://doi.org/10.1007/978-3-642-02295-1_2.
[61] S. Pancratz, *Computing Gauss–Manin connections for families of projectives hypersurfaces*. 2010.
[62] S. Pancratz and J. Tuitman, *Improvements to the deformation method for counting points on smooth projective hypersurfaces*, Found. Comput. Math., 15 (2015), pp. 1413–1464.
[63] F. Pham, *Formules de Picard-Lefschetz généralisées et ramification des intégrales*, Bull. Soc. Math. France, 93 (1965), pp. 333–367.
[64] E. Picard, *Sur les périodes des intégrales doubles et sur une classe d'équations différentielles linéaires*, in Comptes Rendus Hebdomadaires Des Séances de l'Académie Des Sciences, Gauthier-Villars, ed., vol. 134, MM. les secrétaires perpétuels, 1902, pp. 69–71.
[65] B. Poonen, D. Testa, and R. van Luijk, *Computing Néron–Severi groups and cycle class groups*, Compos. Math., 151 (2015), pp. 713–734, https://doi.org/10.1112/S0010437X14007878.
[66] K. Ranestad and C. Voisin, *Variety of power sums and divisors in the moduli space of cubic fourfolds*, Doc. Math., 22 (2017), pp. 455–504.
[67] W. M. Schmidt, *Linear forms with algebraic coefficients. I*, J. Number Theory, 3 (1971), pp. 253–277, https://doi.org/10.1016/0022-314X(71)90001-1.
[68] E. C. Sertöz, *Computing periods of hypersurfaces*. to appear in Mathematics of Computation, https://doi.org/10.1090/mcom/3430, https://arxiv.org/abs/1803.08068.
[69] T. Shioda, *An explicit algorithm for computing the Picard number of certain algebraic surfaces*, Amer. J. Math., 108 (1986), pp. 415–432.
[70] T. Shiota, *Characterization of Jacobian varieties in terms of soliton equations*, Invent. Math., 83 (1986), pp. 333–382.
[71] A. J. Sommese, J. Verschelde, and C. W. Wampler, *Numerical Decomposition of the Solution Sets of Polynomial Systems into Irreducible Components*, SIAM J. Numer. Anal., 38 (2001), pp. 2022–2046,

https://doi.org/10.1137/S0036142900372549.
[72] The LMFDB Collaboration, *The l-functions and modular forms database*. http://www.lmfdb.org, 2013. [Online; accessed 16 September 2013].
[73] The Sage Developers, *SageMath, the Sage Mathematics Software System (Version 8.4)*, 2018.
[74] I. Todorov, *Number theory meets high energy physics*, Phys. Part. Nuclei Lett., 14 (2017), pp. 291–297, https://doi.org/10.1134/S1547477117020339.
[75] P. Tretkoff, *Periods and special functions in transcendence*, Advanced Textbooks in Mathematics, World Scientific Publishing Co. Pte. Ltd., Hackensack, NJ, 2017.
[76] J. van der Hoeven, *Fast evaluation of holonomic functions near and in regular singularities*, J. Symb. Comput., 31 (2001), pp. 717–743, https://doi.org/10.1006/jsco.2000.0474.
[77] J. van der Hoeven, *On effective analytic continuation*, Math. Comput. Sci., 1 (2007), pp. 111–175, https://doi.org/10.1007/s11786-007-0006-6.
[78] R. van Luijk, *K3 surfaces with Picard number one and infinitely many rational points*, Algebra Number Theory, 1 (2007), pp. 1–15, https://doi.org/10.2140/ant.2007.1.1.
[79] P. van Wamelen, *Examples of genus two CM curves defined over the rationals*, Math. Comput., 68 (1999), pp. 307–321, https://doi.org/10.1090/S0025-5718-99-01020-0.
[80] P. Vanhove, *The physics and the mixed Hodge structure of Feynman integrals*, in Proceedings of Symposia in Pure Mathematics, R. Donagi, M. Douglas, L. Kamenova, and M. Rocek, eds., vol. 88, American Mathematical Society, Providence, Rhode Island, Dec. 2014, pp. 161–194, https://doi.org/10.1090/pspum/088/01455.
[81] C. Voisin, *The Hodge conjecture*, in Open problems in mathematics, Springer, 2016, pp. 521–543.
[82] Y. G. Zarhin, *Hodge groups of K3 surfaces*, J. Reine Angew. Math., 341 (1983), pp. 193–220.
[83] O. Zariski, *Algebraic surfaces*, Classics in Mathematics, Springer-Verlag, Berlin, 1995. Reprint of the second (1971) edition.